Synthesis of Bi- and Trinuclear Bis(alkynyl) Complexes [PtM (M = Rh, Ir), $PtRh_2$] Starting from [*cis*-$Pt(C_6F_5)_2(C{\equiv}CR)_2]^{2-}$

Irene Ara,[†] Jesús R. Berenguer,[‡] Eduardo Eguizábal,[‡] Juan Forniés,*[,†] Elena Lalinde,*[,‡] and Francisco Martínez[†]

Departamento de Química Inorgánica, Instituto de Ciencia de Materiales de Aragón, Universidad de Zaragoza-Consejo Superior de Investigaciones Científicas, 50009 Zaragoza, Spain, and Departamento de Química, Universidad de La Rioja, 26001 Logroño, Spain

Received April 29, 1999

The course of the reactions of Q_2[*cis*-$Pt(C_6F_5)_2(C{\equiv}CR)_2$] (Q = PPh_3Me, R = Ph **1a**; Q = NBu_4, R = ^{t}Bu **1b**, $SiMe_3$ **1c**) with [M(μ-Cl)(COD)]$_2$ (M = Rh, Ir) is strongly influenced by the metal and the substituents, as well as the stoichiometry. Thus, whereas treatment of **1a** with either 0.5 or 1 equiv of [Rh(μ-Cl)(COD)]$_2$ gives the chelating-type binuclear highly polar compound (PPh_3Me)[*cis*-$Pt(C_6F_5)_2(\mu$-1κC^{α}:η^2-$C{\equiv}CPh)_2Rh(COD)$], **2a**, analogous reactions using **1b** as the precursor afford only the trinuclear complex (NBu_4)[{*cis*-$Pt(C_6F_5)_2(\mu$-1κC^{α}:η^2-$C{\equiv}C^tBu)_2$}{$Rh_2(\mu$-Cl)$(COD)_2$}], **4b**. On the other hand, related bi- and trinuclear $SiMe_3$ derivatives (NBu_4)[*cis*-$Pt(C_6F_5)_2(\mu$-1κC^{α}:η^2-$C{\equiv}CSiMe_3)_2Rh(COD)$], **2c**, and ($NBu_4$)[{*cis*-$Pt(C_6F_5)_2(\mu$-1$\kappa C^{\alpha}$:$\eta^2$-$C{\equiv}CSiMe_3)_2$}{$Rh_2(\mu$-Cl)$(COD)_2$}], **4c**, are easily obtained by treating **1c** with the binuclear rhodium substrate in the adequate molar ratio [1:0.5 for **2c**; 1:1 for **4c**]. Complex **2b** and, alternatively, **2a**,**c** derivatives can be produced by reacting **1** with the cationic solvento species [Rh(COD)$(Et_2O)_x$]$^+$ (prepared in situ). The molecular structures of **2a** and **4b** have been confirmed by X-ray diffraction. By contrast, whereas the reactions of **1a**,**b** with [Ir(μ-Cl)(COD)]$_2$ lead to the formation of undefined products, the heterobinuclear σ,π double-alkynyl-bridged complex (NBu_4)[*cis*-$Pt(C_6F_5)_2(\mu$-1κC^{α}:η^2-$C{\equiv}CSiMe_3)(\mu$-η^2:2κC^{α}-$C{\equiv}CSiMe_3)Ir(COD)$], **3c**, (X-ray) is isolated from reaction of **1c** with the dimer iridium complex regardless of the molar ratio used (1:0.5 or 1:1).

Introduction

The chemistry of metal alkynyl complexes is an intensely researched area, particularly due to the versatile reactivity of the unsaturated fragment and its wide variety of modes of interaction with transition metals.[1−3] In this area, homo and hetero double-alkynyl-bridged complexes[4−7] have gained particular significance as frozen structures at various points on the reaction paths for either C−C bond coupling alkynide processes[6a,8] or C−C bond cleavage on butadiynes[6b−f,7a,9] mediated by metal centers (Scheme 1).[10,11]

Binuclear M(μ-$C{\equiv}CR)_2M'$ compounds have been prepared through the activation and cleavage of the central C−C single bond of R−C≡C−C≡C−R with "Cp_2M" (M = Ti, Zr) fragments,[6b−f,7a,9] but the most widely used route is based on the addition of a second metal fragment "L_nM'" to a M−σ-bis(alkynyl) compound. Usually, in the resulting complexes, the $L_nM(C{\equiv}CR)_2$ compound used as the starting material acts as a chelating ligand toward the second metal center, forming planar (tweezer-like) or hinged (V-shaped) M_2C_4 central cores (**B**, Scheme 1).[2c,4,7] However, monoalkynyl transfer processes yielding type **C** symmetrical or

[†] Universidad de Zaragoza-Consejo Superior de Investigaciones Científicas.

[‡] Universidad de La Rioja.

(1) (a) Nast, R. *Coord. Chem. Rev.* **1982**, *47*, 89. (b) Carty, A. J. *Pure Appl. Chem.* **1982**, *54*, 113. (c) Sappa, E.; Tiripicchio, A.; Braunstein, P. *Coord. Chem. Rev.* **1985**, *65*, 219. (d) Akita, M.; Moro-Oka, Y. *Bull. Chem. Soc. Jpn.* **1995**, *68*, 420. (e) Forniés, J.; Lalinde, E. *J. Chem. Soc., Dalton Trans.* **1996**, 2587, and references therein. (f) Manna, J.; John, K. D.; Hopkins, M. D. *Adv. Organomet. Chem.* **1995**, *38*, 79.

(2) (a) Beck, V.; Niemer, B.; Wieser, M. *Angew. Chem., Int. Ed. Engl.* **1993**, *32*, 923. (b) Lotz, S.; Van Rooyen, P. H.; Meyer, R. *Adv. Organomet. Chem.* **1995**, *37*, 219. (c) Lang, H.; Köhler, K.; Blau, S. *Coord. Chem. Rev.* **1995**, *143*, 113.

(3) (a) Bruce, M. I. *Chem. Rev.* **1991**, *91*, 197. (b) Davies, S. G.; McNally, J. P.; Smallridge, A. J. *Adv. Organomet. Chem.* **1990**, *30*, 1. (c) Werner, H. *J. Organomet. Chem.* **1994**, *475*, 45. (d) Werner, H. *J. Chem. Soc., Chem. Commun.* **1997**, 903. Some recent works: (e) George, D. S. A.; McDonald, R.; Cowie, M. *Organometallics* **1998**, *17*, 2553. (f) Leininger, S.; Stang, P. *Organometallics* **1998**, *17*, 3981. (g) Wong, W.-Y.; Wong, W.-K.; Raithby, P. R. *J. Chem. Soc., Dalton Trans.* **1998**, 2761. (h) Uno, M.; Dixneuf, P. H. *Angew. Chem., Int. Ed. Engl.* **1998**, *37*, 1714. (i) Pin, Ch.-W.; Chi, Y.; Chung, C.; Carty, A. J.; Peng, S.-M.; Lee, G.-H. *Organometallics* **1998**, *17*, 4146. (j) Bruce, M. I.; Ke, M.; Low, P. J.; Skelton, B. W.; White, A. H. *Organometallics* **1998**, *17*, 3539. (k) Falloon, S. B.; Szafert, S.; Arif, A. M.; Gladysz, J. A. *Chem. Eur. J.* **1998**, *4*, 1033. (l) de los Ríos, I.; Tenorio, M. J.; Puerta, M. C.; Valerga, P. *Organometallics* **1998**, *17*, 3356. (m) Yi, Ch. S.; Lin, N. *Organometallics* **1998**, *17*, 3158. (n) Buttinelli, A.; Viola, E.; Antonelli, E.; Lo Sterzo, C. *Organometallics* **1998**, *17*, 2574. (o) Long, N. J.; Martin, A. J.; de Biani, F. F.; Zanello, P. *J. Chem. Soc., Dalton Trans.* **1998**, 2017. (p) Guillemott, M.; Tonpet, L.; Lapinte, C. *Organometallics* **1998**, *17*, 1928. (q) Blake, R. F., Jr.; Antonelli, D. M.; Henling, L. M.; Schaefer, W. P.; Hardcastle, K. I.; Bercaw, J. E. *Organometallics* **1998**, *17*, 718. (r) Gamasa, M. P.; Gimeno, J.; Martín-Vaca, B. M. *Organometallics* **1998**, *17*, 3707. (s) Crochet, P.; Esteruelas, M. A.; Gutiérrez-Puebla, E. *Organometallics* **1998**, *17*, 3141. (t) Roth, G.; Reindl, D.; Gockel, M.; Troll, C.; Fisher, H. *Organometallics* **1998**, *17*, 1393. (u) Gil-Rubio, J.; Laubender, M.; Werner, H. *Organometallics* **1998**, *17*, 1202. (v) Vaid, T. M.; Veige, A. S.; Lobkovsky, E. B.; Glassey, W. V.; Wolczanski, P. T.; Liable-Sands, L. M.; Rheingold, A. L.; Cundari, T. R. *J. Am. Chem. Soc.* **1998**, *120*, 10067.

(4) Ara, I.; Berenguer, J. R.; Forniés, J.; Lalinde, E. *Inorg. Chim. Acta* **1997**, *264*, 199, and references therein.

10.1021/om990314z CCC: $18.00
Publication on Web 09/23/1999

unsymmetrical σ/π bridging systems (Scheme 1) have also been reported.[6g−i,k,q,12] We have recently reported a new family of bis(μ-C≡CR) binuclear [(PEt_3)Cp*M(μ-C≡CR)$_2$M′(C_6F_5)$_2$] d^6(Rh, Ir)−d^8(Pt, Pd) complexes.[11,13] The Ir−Pt complexes (chelating type, V-shape) were prepared by an unprecedented double intramolecular alkynyl migration from Pt to Ir, whereas the analogous Rh derivatives (σ/π) were formed through a unique

Scheme 1

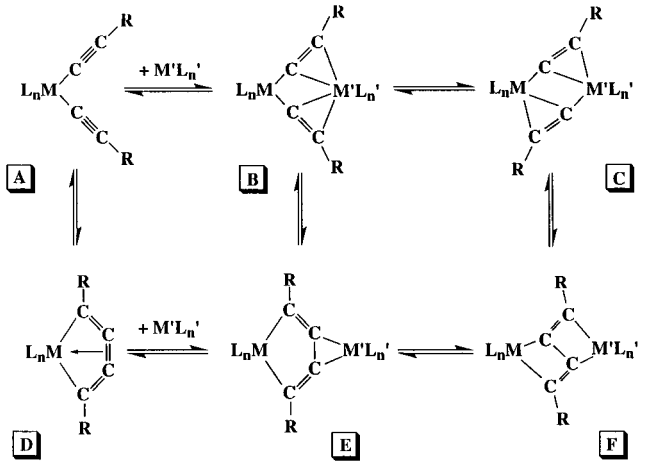

alkynyl migration, either from Pt to Rh or from Rh to Pt. A double alkynyl migration has also been recently suggested by Choukroun et al.[14] to explain the formation of the coupled product [$Cp_2V(\mu$-η^2:η^4-butadiyne)MCp'_2] (Cp′ = Cp, M = Ti, Zr; Cp′ = $C_5H_4SiMe_3$, M = Zr) (**E**, Scheme 1) starting from [$Cp_2M(C{\equiv}CPh)_2$] and vanadocene and could also be related to the oxidatively induced coupling of C≡CR moieties to free butadiynes (eq 1), only observed with very electrophilic ML_n fragments[15] (Ni(II) or Pd(II) vs Ni(0) or Pd(0); $AuCl_3$py vs AuR or $AgPF_6$).

$$L_mM'(C{\equiv}CR)_2 + ML_n \rightarrow L_mM'L_n + M(0) + RC{\equiv}C{-}C{\equiv}CR \quad (1)$$

The driving force of these alkynyl transfer processes is still an open question.[6g−i,k,12,16] With this in mind, we have studied the reactivity of alkynyl platinum complexes toward low-valence substrates of Rh or Ir(I), and the synthesis and characterization of several new bi- and trinuclear bis(alkynyl)-bridged [PtM, M = Rh, Ir; $PtRh_2$] complexes are reported.

Results and Discussion

Preparation of Complexes. We have recently shown that treatment of the allyl chloride-bridged dimer [Pd(μ-Cl)(η^3-C_3H_5)]$_2$ with the anionic platinum complexes Q_2[*cis*-Pt(C_6F_5)$_2$(C≡CR)$_2$] **1** (Q = PPh_3Me, R = Ph; Q = NBu_4, R = ^{t}Bu, $SiMe_3$) provides an excellent route to the heterobinuclear double-alkynyl V-shaped anionic derivatives [{*cis*-Pt(C_6F_5)$_2$(μ-C≡CR)$_2$}{Pd(η^3-C_3H_5)}]$^-$ [17] (**B**, Scheme 1). In these reactions the chloride ligands are easily displaced as NBu_4Cl or PPh_3MeCl. These results led us to investigate the reactivity of **1** toward the chloride-bridged dimers [M(μ-Cl)(COD)]$_2$ (M = Rh, Ir) as a reasonable route to the desired alkynyl bridging Pt−M (M = Rh, Ir) compounds. These reactions display a surprising dependence on the nature of M, the alkynyl organic substituent R, and the proportions of the reagents as summarized in Scheme 2. The expected

(5) (μ-1κC^α: 2κC^α-C≡CR)$_2$: (a) Erker, G.; Albrecht, M.; Krüger, C.; Nolte, M.; Werner, S. *Organometallics* **1993**, *12*, 4979, and references therein. (b) Berenguer, J. R.; Falvello, L. R.; Forniés, J.; Lalinde, E.; Tomás, M. *Organometallics* **1993**, *12*, 6. (c) Duchateau, R.; van Wee, C. T.; Meetsma, A.; Teuben, J. H. *J. Am. Chem. Soc.* **1993**, *115*, 4931. (d) Yam, V. W.-W.; Lee, W.-K.; Cheung, K. K.; Lee, H.-K.; Leung, W.-P. *J. Chem. Soc., Chem. Commun.* **1996**, 2889. (e) Edwards, A. J.; Paver, M. A.; Raithby, P. R.; Rennie, M. A.; Russell, C. A.; Wright, D. S. *Organometallics* **1994**, *13*, 4967. (f) Olbrich, F.; Behrems, U.; Weiss, E. *J. Organomet. Chem.* **1994**, *472*, 365.

(6) (μ-1κC^α:η^2-C≡CR)(μ-2κC^α:η^2-C≡CR): (a) Cuenca, T. M.; Gómez, R.; Gómez-Sal, P.; Rodríguez, G. M.; Royo, P. *Organometallics* **1992**, *11*, 1229. (b) Burlakov, V. V.; Ohff, A.; Lefeber, C.; Tillack, A.: Baumann, W.; Kempe, R.; Rosenthal, U. *Chem. Ber.* **1995**, *128*, 967. (c) Varga, V.; Mach, K.; Hiller, J.; Thewalt, U.; Sedmera, P.; Polásek, M. *Organometallics* **1995**, *14*, 1410. (d) Rosenthal, U.; Pulst, S.; Arndt, P.; Ohff, A.; Tillack, A.; Baumann, W.; Kempe, R.; Burlakov, V. V. *Organometallics* **1995**, *14*, 2961, and references therein. (e) Rosenthal, U.; Ohff, A.; Baumann, W.; Kempe, R.; Tillack, A.; Burlakov, V. V. *Organometallics* **1994**, *13*, 2903. (f) Rosenthal, U.; Gorls, H. *J. Organomet. Chem.* **1992**, *439*, C36. (g) Erker, G.; Frömberg, W.; Benn, R.; Mynnott, R.; Agermund, K.; Krüger, C. *Organometallics* **1989**, *8*, 911. (h) Berenguer, J. R.; Forniés, J.; Martínez, F.; Cubero, J.; Lalinde, E.; Moreno, M. T.; Welch, A. J. *Polyhedron* **1993**, *12*, 1797. (i) Forniés, J.; Gómez-Saso, M. A.; Lalinde, E.; Martínez, F.; Moreno, M. T. *Organometallics* **1992**, *11*, 2873. (j) Muller, J.; Tschampell, M.; Pickardt, J. *J. Organomet. Chem.* **1988**, *355*, 513. (k) Erker, G.; Frömberg, W.; Mynott, R.; Gabor, B.; Krüger, C. *Angew. Chem., Int. Ed. Engl.* **1986**, *25*, 463. (l) Lang, H.; Blau, S.; Nuber, B.; Zsolnai, L. *Organometallics* **1995**, *14*, 3216. (m) Metzler, N.; Nöth, H. *J. Organomet. Chem.* **1993**, *454*, C5. (n) Heshmatpour, F.; Wocadlo, S.; Massa, W.; Dehnicke, K. *Acta Crystallogr.* **1995**, *C51*, 2225. (o) Wood, G. L.; Knobler, C. B.; Hawthorne, M. F. *Inorg. Chem.* **1989**, *28*, 382. (p) Mihan, S.; Weidmann, T.; Weinrich, V.; Fenske, D.; Beck, W. *J. Organomet. Chem.* **1997**, *541*, 423. (q) Schottek, J.; Erker, G.; Fröchlich, R. *Eur. J. Inorg. Chem.* **1998**, 551.

(7) (μ-1κC^α:η^2-C≡CR)$_2$: (a) Troyanov, S. I.; Varga, V.; Mach, K. *Organometallics* **1993**, *12*, 2820. (b) Janssen, M. D.; Herres, M.; Dedieu, A.; Smeets, W. J. J.; Spek, A. L.; Grove, D. M.; Lang, H.; Van Koten, G. *J. Am. Chem. Soc.* **1996**, *118*, 4817, and references therein. (c) Yamazaki, S.; Deeming, A. J. *J. Chem. Soc., Dalton Trans.* **1993**, 3051. (d) Berenguer, J. R.; Forniés, J.; Lalinde, E.; Martín, A.; Moreno, M. T. *J. Chem. Soc., Dalton Trans.* **1994**, 3343. (e) Ara, I.; Fernández, S.; Forniés, J.; Lalinde, E.; Martín, A.; Moreno, M. T. *Organometallics* **1997**, *16*, 5923. (f) Lang, H.; Köhler, K.; Zsolnai, L. *J. Chem. Soc., Chem. Commun.* **1996**, 2043. (g) Lang, H.; Wu, I.-Y.; Weinman, S.; Weber, Ch.; Nuber, B. *J. Organomet. Chem.* **1997**, *541*, 157. (h) Lang, H.; Weinmann, M. *Synlett* **1996**, 1, and references therein. (i) Zhang, D.; McConville, D. B.; Hrabusa, J. M.; Tessier, C. A.; Youngs, W. J. *J. Am. Chem. Soc.* **1998**, *120*, 3506.

(8) (a) Sekutowski, D. G.; Stucky, G. D. *J. Am. Chem. Soc.* **1976**, *98*, 1376. (b) Evans, W. J.; Keyer, R. A.; Ziller, J. W. *Organometallics* **1990**, *9*, 2628. (c) Evans, W. J.; Keyer R. A.; Ziller, J. W. *Organometallics* **1993**, *12*, 2618. (d) Forsyth, C. M.; Nolan, S. P.; Stern, C. L.; Marks, T. J.; Rheingold, A. L. *Organometallics* **1993**, *12*, 3618. (e) Heeres, H. J.; Nijholf, J.; Teuben, J. H.; Rogers, R. D. *Organometallics* **1993**, *12*, 2609. (f) Duchateau, R.; van Wee, C. T.; Teuben, J. H. *Organometallics* **1996**, *15*, 2291. (g) Lee, L.; Berg, D. J.; Bushnell, G. W. *Organometallics* **1995**, *14*, 5021. (h) Takahashi, T.; Xi, Z.; Obora, Y.; Suzuki, N. *J. Am. Chem. Soc.* **1995**, *117*, 2665.

(9) (a) Pellny, P.-M.; Peulecke, N.; Burlakov, V., V.; Tillack, A.; Baumann, W.; Spanneberg, A.; Kempe, R.; Rosenthal, U. *Angew. Chem., Int. Ed. Engl.* **1997**, *36*, 2615. (b) Pulst, S.; Arndt, P.; Heller, B.; Baumann, W.; Kempe, R.; Rosenthal, H. *Angew. Chem., Int. Ed. Engl.* **1996**, *35*, 1112, and references therein. (c) Rosenthal, U.; Ohff, A.; Tillack, A.; Baumann, W.; Görls, H. *J. Organomet. Chem.* **1994**, *488*, C4. (d) Hsu, P. D.; Davis, W. M.; Buchwald, S. L. *J. Am. Chem. Soc.* **1993**, *115*, 10394.

(10) (a) Pavan Kumar, P. N. V.; Jemmis, E. D. *J. Am. Chem. Soc.* **1988**, *110*, 125. (b) Jemmis, E. D.; Gijn, K. T. *Angew. Chem., Int. Ed. Engl.* **1997**, *36*, 606. (c) Ibid. *J. Am. Chem. Soc.* **1998**, *120*, 6952.

(11) Ara, I.; Berenguer, J. R.; Eguizábal, E.; Forniés, J.; Lalinde, E.; Martín, A.; Martínez, F. *Organometallics* **1998**, *17*, 4578.

(12) Berenguer, J. R.; Forniés, J.; Lalinde, E.; Martín, A. *Angew. Chem., Int. Ed. Engl.* **1994**, *33*, 2083.

(13) Berenguer, J. R.; Forniés, J.; Lalinde, E.; Martínez, F. *J. Chem. Soc., Chem. Commun.* **1995**, 1227.

(14) Danjoy, C.; Zhao, J.; Donnadieu, B.; Legros, J.-P.; Valade, L.; Choukron, R.; Zwick, A.; Cassoux, P. *Chem. Eur. J.* **1998**, *4*, 1100.

(15) (a) Köhler, K.; Silverio, S. J.; Hyla-Kryspin. I.; Gleiter, R.; Zsolnai, L.; Driess, A.; Huttner, G.; Lang, H. *Organometallics* **1997**, *16*, 4970. (b) Back, S.; Pritzkow, H.; Lang, H. *Organometallics* **1998**, *17*, 41. (c) Hayashi, Y.; Osawa, M.; Wakatsuki, Y. *J. Organomet. Chem.* **1997**, *542*, 241. (d) Ibid. *J. Chem. Soc., Chem. Commun.* **1996**, 1617.

Scheme 2

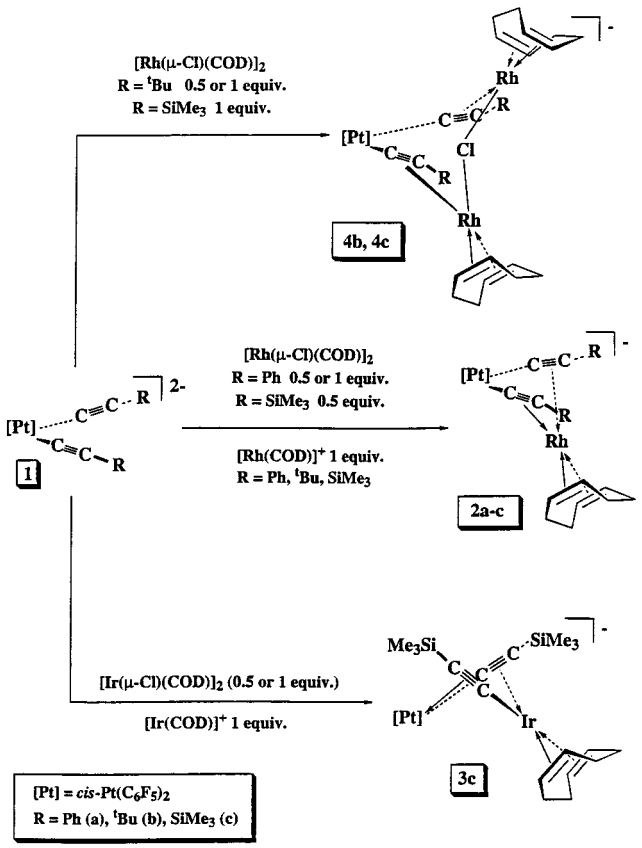

heterobinuclear platinum−rhodium complexes Q[*cis*-Pt-$(C_6F_5)_2(\mu$-C≡CR$)_2$Rh(COD)] (Q = PPh_3Me, R = Ph **2a**; Q = NBu_4, R = $SiMe_3$ **2c**) can be isolated, as orange solids, in good (81%, **2a**) or moderate (42%, **2c**) yield by the reaction of [Rh(μ-Cl)(COD)]$_2$ with 2 equiv of **1a** and **1c**, respectively (Rh/Pt, 1:1 ratio). As expected, both complexes can also be obtained directly by the reaction of **1a** and **1c** with the solvento species [Rh(COD)S_2]-(ClO_4) in diethyl ether. The analogous *tert*-butylalkynyl derivative **2b** can only be synthesized (64% yield) starting from [Rh(COD)S_2]$^+$ (S = diethyl ether) and the corresponding *tert*-butylalkynyl platinum precursor **1b**. Attempts to synthesize **2b** by the reaction of [Rh(μ-Cl)-(COD)]$_2$ with 2 molar equiv of **1b** lead to the trinuclear anionic complex (NBu_4)[{*cis*-Pt(C_6F_5)$_2$(μ-C≡C^{t}Bu)$_2$}{Rh_2-(μ-Cl)(COD)$_2$}], **4b**, instead. This is isolated in low yield (56% based on Rh) as a microcrystalline orange solid. If the reaction is carried out in a 1:1 molar ratio, complex **4b** is generated in higher yield (67%). The reaction of [Rh(μ-Cl)(COD)]$_2$ with 1 equiv of **1c** also results in the displacement of one of the chloride ligands to afford the analogous trinuclear **4c**. In these **4b**,**c** complexes, as has been shown by an X-ray diffraction study on **4b**, the bis(alkynyl)platinate precursor acts as a bidentate bridging ligand replacing one chloride group in the rhodium chloride-bridged dimer. Attempts to obtain the phenyl derivative **4a** using the appropiate platinum−rhodium molar ratio were unsuccessful, and instead, after workup, an orange solid which is identified (IR and NMR spectroscopy) as a mixture of the dimer **2a** and unreacted [Rh(μ-Cl)(COD)]$_2$ (2.5:1) is obtained. No other product can be detected by NMR techniques. The formulation given in Scheme 2 for complexes **2** and **4** is based on spectroscopic data (IR, ^{1}H, ^{19}F, ^{13}C NMR) and confirmed by X-ray diffraction studies of complexes **2a** and **4b**, respectively. All complexes have been additionally characterized by elemental analyses, mass spectrometry (FAB), and conductivity measurements (see Experimental Section).

As it is shown in the formulas that appear in Scheme 2, no alkynylation processes have been observed in the formation of complexes **2** and **4**. The platinum centers retain the σ-coordination to the alkynyl fragments while the rhodium centers are stabilized through η^2-alkyne interactions, indicating that, as expected for a third-row metal, the platinum center shows a greater preference for the σ-electron density than the Rh center does.

In contrast to the behavior observed in relation to the rhodium species, we were able to obtain only a mixed-metal binuclear species stabilized by a double alkynyl-bridging system by the reaction of **1c** and the dimeric iridium complex [Ir(μ-Cl)(COD)$_2$]. As shown in Scheme 2, the Ir−Pt complex (NBu_4)[*cis*-Pt(C_6F_5)$_2$(μ-C≡C$SiMe_3$)$_2$-Ir(COD)], **3c**, is readily obtained as a deep yellow microcrystalline solid by reacting **1c** with the chloride-dimer iridium complex in acetone, regardless of the Pt/Ir ratio used (1:0.5 31% yield; 1:1 65% yield). Complex **3c** is also generated in very good yield, as is observed by NMR spectroscopy (^{19}F), by mixing equimolar amounts of **1c** and the solvento [Ir(COD)S_2](ClO_4) species in acetone. However, due to the presence of NBu_4ClO_4 in the reaction mixture, **3c** can be isolated as a pure compound only in extremely low yield (15%). All attempts to prepare any other alkynyl-bridged Pt(II)−Ir-(I) dimer (or trimer) using **1a** and **1b** as the reagents for the Ir derivatives have been unsuccessful. The reaction mixtures of **1a**,**b** with either [Ir(μ-Cl)(COD)]$_2$ or [Ir(COD)S_2]$^+$ evolve giving a complex mixture of products from which we were not able to isolate any pure compound. Interestingly, NMR examination of the initial reaction mixture of **1a** and [Ir(μ-Cl)(COD)]$_2$ (1:0.5 or 1:1 molar ratio) reveals the presence of the doubly alkynyl bridged diplatinum complex $(PPh_3Me)_2$[Pt(μ-C≡CPh)(C_6F_5)$_2$]$_2$,[6i] suggesting that, in this case, after initial alkynyl transfer from Pt to Ir, the resulting fragments probably disproportionate, producing the diplatinum and presumably the dimer [Ir(μ-C≡CPh)(COD)]$_2$. By usual workup (see Experimental Section) an orange solid was obtained and identified (NMR) as a mixture of products, with the known dimer $(PPh_3Me)_2$[Pt(μ-C≡CPh)(C_6F_5)$_2$]$_2$ as the major component.

For complex **3c**, the formulation given with a type **C** σ/π double-alkynyl bridging system (Scheme 1) coincides with its spectroscopic data (IR, NMR) and has been confirmed by a single-crystal X-ray diffraction study.

(16) (a) Forniés, J.; Lalinde, E.; Martín, A.; Moreno, M. T. *J. Chem. Soc., Dalton Trans.* **1994**, 135. (b) Berenguer, J. R.; Forniés, J.; Lalinde, E.; Martínez, F.; Urriolabeitia, E.; Welch, A. J. *J. Chem. Soc., Dalton Trans.* **1994**, 1291. (c) Ipaktschi, J.; Mirzaei, F.; Müller, B. G.; Beck, J.; Serafin, M. *J. Organomet. Chem.* **1996**, *526*, 363. (d) Akita, M.; Ishii, N.; Takabuchi, A.; Tanaka, M.; Moro-Oka, Y. *Organometallics* **1994**, *13*, 258. (e) Fritz, P. M.; Polborn, K.; Steinman, M.; Beck, W. *Chem. Ber.* **1989**, *122*, 889. (f) Bruce, M. I.; Abu-Salah, O. M.; Davis, P. E.; Raghavan, N. V. *J. Organomet. Chem.* **1974**, *64*, C48. (g) Lai, N.-S.; Tu, W.-Ch.; Peng, S.-M.; Lee, G.-H. *Organometallics* **1994**, *13*, 4652. (h) Ara, I.; Berenguer, J. R.; Forniés, J.; Lalinde, E.; Tomás, M. *Organometallics* **1996**, *15*, 1014. (i) Berenguer, J. R.; Forniés, J.; Lalinde, E.; Martínez, F. *Organometallics* **1995**, *14*, 2532.

(17) (a) Berenguer. J. R.; Forniés, J.; Lalinde, E.; Martínez, F. *J. Organomet. Chem.* **1994**, *470*, C15. (b) Ibid. *Organometallics* **1996**, *15*, 4537.

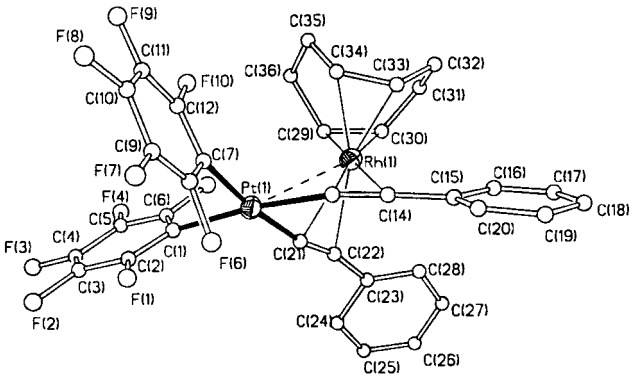

Figure 1. Molecular structure of the anion complex **2a**, showing the atom-numbering scheme.

This well-studied bridging system has been found to stabilize both early (d^1-d^1),[6a−c,e−g,k−o,q] middle(d^6-d^6),[6p] and late (d^8-d^8)[6h−j] transition metal homobinuclear molecules, but the number of heterodimetallic systems is rather scarce.[6b,d,11,12] As far as we know, the only related metal complexes (Pt, Rh, or Ir) previously reported are the dimers $[(COD)M(C{\equiv}CSiMe_3)]_2$ [M = Ir (X-ray), Rh],[6j] and we have also shown that anionic $\{[Pt(C{\equiv}CR)(C_6F_5)_2]_2\}^{2-}$[6i] and neutral $[Pt(C{\equiv}CR)(C_6F_5)(PPh_3)]_2$[6h] binuclear complexes display a similar structural disposition. Complex **3c** represents the first heterobimetallic d^8-d^8 compound characterized by an X-ray diffraction study that also possesses a σ/π doubly alkynyl bridging system. The formation of **3c** implies the migration of one σ-$C{\equiv}CSiMe_3$ group from Pt to Ir. However, the migration of the second alkynyl ligand, previously observed in the reaction between $[cis\text{-}Pt(C_6F_5)_2(C{\equiv}CR)_2]^{2-}$ and $[Cp^*Ir(PEt_3)(acetone)_2]^{2+}$,[11] is not observed with the "$Ir(COD)^+$" fragment.

Structural Investigations. The structures of complexes **2a**, **3c**, and **4b** have been established by an X-ray crystal study. The drawing of complex anion $[cis\text{-}Pt(C_6F_5)_2(\mu\text{-}C{\equiv}CPh)_2Rh(COD)]^-$, **2a**, is presented in Figure 1, and selected bond distances and angles are given in Table 1. The type of structure with a chelating doubly alkynyl bridging system (**B**, Scheme 1) is not new, but, to the best of our knowledge, this is the first example involving these metal centers [Pt(II) and Rh(I)]. We have recently described the Pt(II)−Rh(III) binuclear zwitterionic neutral complex $[(PEt_3)Cp^*Rh^+(\mu\text{-}C{\equiv}CSiMe_3)_2Pt^-(C_6F_5)_2]$, but it contains a σ/π bis(alkynyl) system (**C**, Scheme 1).[11] In **2a** both alkynyl groups are σ-bonded to the platinum atom [Pt(1)−C(13) 2.02(2) Å, Pt(1)−C(21) 2.04(3) Å] and η^2-bonded to the rhodium center, resulting in a very polar anion (formally zwitterionic). It has to be mentioned that the final arrangement around the rhodium atom is actually new. Athough there is a large number of examples of η^2-acetylene−rhodium bonds,[18] the easy activation of the alkynes coordinated to rhodium centers to give metallacyclopentadiene[19] and cyclobutadiene[18a,20] complexes has precluded the isolation of derivatives with a rhodium atom η^2-bonded to two alkyne ligands. We have recently reported two similar complexes,[21] but this structure represents the first crystallographically characterized example of this structural situation.

The platinum and rhodium atoms exhibit conventional square-planar environments, and each organometallic core shows the expected structural features.[4,11,13,16a,17a,21,22] The rhodium atom is located out of the 3-metalla-1,4-diyne plane (V-shape). We have previously observed this structural feature when using square-planar d^8 metal moieties as chelating fragments.[6i,7e,11,13,16a,17,21] The dihedral angle formed by the best least-squares planes around the Pt and Rh atoms [96.86(1)°] is notably smaller than those found for other related complexes [121.54(6)−148.3(4)°],[6i,7e,13,16a] allowing the metal centers to be in a closer position. Finally, the π-interactions between the acetylene fragments and the Rh atom are rather unsymmetrical [Rh−C_α 2.29(2) Å, 2.29(3) Å; Rh−C_β 2.53(3) Å, 2.49(2) Å]. This type of asymmetry (Rh−C_α < Rh−C_β bond distances), although not as marked, has been previously found in the pentanuclear species $[\{Pt(C{\equiv}C^tBu)_4\}\{Rh_2(\mu\text{-}X)(COD)_2\}_2]$ (X = OH, Cl), **[PtRh$_4$X$_2$]**, previously reported[21] and in related complexes containing η^2-Rh−acetylide interactions.[23]

The structure of the dimetallic anion of **3c** is shown in Figure 2 together with the atom-numbering scheme. Selected bond distances and angles are displayed in Table 1. As can be seen, the anion is formed by two organometallic "(COD)Ir" and "$Pt(C_6F_5)$" moieties [Ir···Pt = 3.639(1) Å] with the metal centers connected by two alkynyl groups. Each alkynyl ligand is σ-bonded to one metal atom (Pt/Ir) and leans over the other metal center (Ir/Pt). All structural data are in good agreement with the structures of the previously reported homobimetallic species $\{[Pt(C{\equiv}CPh)(C_6F_5)_2]_2\}^{2-}$, **[Pt$_2$]**$^{2-}$,[6i] and $[Ir(C{\equiv}CSiMe_3)(COD)]_2$, **[Ir$_2$]**,[6j] which display a similar geometric arrangement of the alkynyl ligands. In particular, the central organometallic framework $IrPtC_4$ adopts a puckered conformation, the dihedral angle between the planes Pt(1)Ir(1)C(18)C(19) and Pt(1)Ir(1)C(1)C(2) being 21.5(3)°. It is worth noting that the influence of the metal centers in the bonding parameters of the Ir(μ-alkynide)$_2$Pt unit is quite insignificant. Thus, both the M−C σ-bonds [1.987(8), 2.005(8) Å] and the equivalent complexed η^2-bond lengths [2.339(8), 2.233-

(18) (a) *Comprehensive Organometallic Chemistry*; Wilkinson, G., Stone, F. G. A., Abel, E. W., Eds.; Pergamon Press Ltd.: Oxford, U.K., 1982; Vol. 5. (b) *Comprehensive Organometallic Chemistry II*; Atwood, J. D., Vol. Ed.; Wilkinson, G., Stone, F. G. A., Abel, E. W., Eds.; Elsevier: Oxford, U.K., 1995; Vol. 8.

(19) (a) Mague, J. T.; Wilkinson, G. *Inorg. Chem.* **1968**, *7*, 542. (b) Müller, E. *Synthesis* **1974**, 761. (c) Winter, W. *Angew. Chem., Int. Ed. Engl.* **1976**, *15*, 241. (d) Sánchez-Delgado, R. A.; Wilkinson, G. *J. Chem. Soc., Dalton Trans.* **1977**, 804. (e) Sünkel, K. *Chem. Ber.* **1991**, *124*, 2449. (f) Bianchini, C.; Masi, D.; Meli, A.; Peruzzini, M.; Vacca, A.; Laschi, F.; Zanello, P. *Organometallics* **1991**, *10*, 636.

(20) (a) Müller, E.; Thomas, R.; Zountsas, G. *Liebigs. Ann. Chem.* **1972**, *758*, 16. (b) Cash, G. G.; Helling, J. F.; Mathew, M.; Palenick, G. J. *J. Organomet. Chem.* **1973**, *50*, 277. (c) Nixon, J. F.; Kooti, M. *J. Organomet. Chem.* **1976**, *104*, 231. (d) King, R. B.; Ackermann, M. N. *J. Organomet. Chem.* **1974**, *67*, 431. (e) Winter, W. *Angew. Chem., Int. Ed. Engl.* **1975**, *14*, 170. (f) Rausch, M. D.; Gardner, S. A.; Tokas, E. F.; Bernal, I.; Reisner, G. M.; Clearfield, A. *J. Chem. Soc., Chem. Commun.* **1978**, 187. (g) Moreto, J.; Maruya, K.; Bailey, P. M.; Maitlis, P. M. *J. Chem. Soc., Dalton Trans.* **1982**, 1341. (h) Borrini, A.; Diversi, P.; Ingrosso, G.; Lucherini, A.; Serra, G. *J. Mol. Catal.* **1985**, *30*, 181.

(21) Ara, I.; Berenguer, J. R.; Forniés, J.; Lalinde, E. *Organometallics* **1997**, *16*, 3921.

(22) (a) Selent, A.; Ramm, M. *J. Organomet. Chem.* **1995**, *485*, 35. (b) Tejel, C.; Villoro, J. M.; Ciriano, M. A.; López, J. A.; Eguizábal, E.; Lahoz, F. J.; Bakhmutov, V. I.; Oro, L. A. *Organometallics* **1996**, *15*, 2967.

(23) Hutton, A. T.; Langrick, C. R.; McEvan, D. M.; Pringle, P. G.; Shaw, B. L. *J. Chem. Soc., Dalton Trans.* **1985**, 2121. (b) Cowie M.; Loeb, S. *Organometallics* **1985**, *4*, 852. (c) Esteruelas, M. A.; Lahuerta, O.; Modrego, J.; Nürnberg, O.; Oro, L. A.; Rodríguez, L.; Sola E.; Werner, H. *Organometallics* **1993**, *12*, 266. (d) Antwi-Nsiah, H. F.; Oke O.; Cowie, M. *Organometallics* **1996**, *15*, 506. (e) George, D. S. A.; McDonald, R.; Cowie, M. *Organometallics* **1998**, *17*, 2553.

Table 1. Selected Bond Lengths (Å) and Angles (deg) for Complexes 2a, 3c, and 4b

Complex **2a**

Pt(1)−C(13)	2.02(2)	Pt(1)−C(21)	2.04(3)	Pt(1)−C(7)	2.08(3)
Pt(1)−C(1)	2.13(3)	Rh(1)−C(33)	2.12(3)	Rh(1)−C(30)	2.12(3)
Rh(1)−C(34)	2.13(3)	Rh(1)−C(29)	2.14(3)	Rh(1)−C(21)	2.29(3)
Rh(1)−C(13)	2.29(2)	Rh(1)−C(22)	2.49(2)	Rh(1)−C(14)	2.53(3)
C(13)−C(14)	1.24(4)	C(21)−C(22)	1.18(4)	C(29)−C(30)	1.44(5)
C(33)−C(34)	1.43(4)	Pt(1)−Rh(1)	2.889(3)		

C(13)−Pt(1)−C(21)	80.6(10)	C(13)−Pt(1)−C(7)	94.6(11)
C(21)−Pt(1)−C(1)	93.2(10)	C(7)−Pt(1)−C(1)	91.9(11)
C(13,14)−Rh(1)−C(21,22)	85.69(2)	C(21,22)−Rh(1)−C(29,30)	97.26(2)
C(29,30)−Rh(1)−C(33,34)	86.98(2)	C(33,34)−Rh(1)−C(13,14)	91.08(2)
C(14)−C(13)−Pt(1)	164(2)	C(13)−C(14)−C(15)	173(3)
C(22)−C(21)−Pt(1)	168(3)	C(21)−C(22)−C(23)	167(3)

Complex **3c**

Pt(1)−C(1)	1.987(8)	Pt(1)−C(6)	2.016(9)	Pt(1)−C(12)	2.054(8)
Pt(1)−C(18)	2.339(8)	Pt(1)−C(19)	2.233(9)	Ir(1)−C(1)	2.308(8)
Ir(1)−C(2)	2.186(9)	Ir(1)−C(18)	2.005(8)	Ir(1)−C(23)	2.199(9)
Ir(1)−C(26)	2.123(10)	Ir(1)−C(27)	2.117(9)	Ir(1)−C(30)	2.199(10)
C(1)−C(2)	1.273(12)	C(18)−C(19)	1.244(12)	Pt(1)···Ir(1)	3.639(1)

C(1)−Pt(1)−C(6)	90.4(3)	C(6)−Pt(1)−C(12)	87.1(3)
C(12)−Pt(1)−C(18,19)	103.4(2)	C(1)−Pt(1)−C(18,19)	79.1(2)
C(1,2)−Ir(1)−C(23,30)	105.3(1)	C(1,2)−Ir(1)−C(18)	80.2(2)
C(18)−Ir(1)−C(26,27)	88.2(2)	C(26,27)−Ir(1)−C(23,30)	86.3(1)
Pt(1)−C(1)−C(2)	174.6(7)	Si(1)−C(2)−C(1)	136.9(7)
Ir(1)−C(18)−C(19)	173.3(7)	Si(2)−C(19)−C(18)	145.0(8)

Complex **4b**

Pt(1)−C(13)	1.995(14)	Pt(1)−C(19)	2.01(2)	Pt(1)−C(1)	2.072(13)
Pt(1)−C(7)	2.076(13)	Rh(1)−C(26)	2.11(2)	Rh(1)−C(30)	2.14(2)
Rh(1)−C(25)	2.14(2)	Rh(1)−C(29)	2.15(2)	Rh(1)−C(13)	2.238(13)
Rh(1)−Cl(1)	2.421(4)	Rh(1)−C(14)	2.500(14)	Rh(2)−C(33)	2.11(2)
Rh(2)−C(34)	2.12(2)	Rh(2)−C(38)	2.15(2)	Rh(2)−C(37)	2.16(2)
Rh(2)−C(19)	2.266(12)	Rh(2)−Cl(1)	2.420(4)	Rh(2)−C(20)	2.547(14)
C(13)−C(14)	1.21(2)	C(19)−C(20)	1.21(2)	C(25)−C(26)	1.43(3)
C(29)−C(30)	1.44(2)	C(33)−C(34)	1.45(3)	C(37)−C(38)	1.44(3)
Pt(1)···Rh(1)	3.238(1)	Pt(1)···Rh(2)	3.206(1)	Rh(1)···Rh(2)	3.670(1)

C(13)−Pt(1)−C(19)	98.1(5)	C(13)−Pt(1)−C(1)	85.9(5)
C(19)−Pt(1)−C(7)	85.2(5)	C(1)−Pt(1)−C(7)	91.0(5)
Cl(1)−Rh(1)−C(13,14)	88.3(2)	Cl(1)−Rh(2)−C(19,20)	87.4(2)
Cl(1)−Rh(1)−C(25,26)	88.1(2)	Cl(1)−Rh(2)−C(33,34)	89.7(2)
C(13,14)−Rh(1)−C(29,30)	95.0(1)	C(19,20)−Rh(1)−C(37,38)	96.8(1)
Rh(2)−Cl(1)−Rh(1)	98.60(14)	C(14)−C(13)−Pt(1)	172.2(12)
C(13)−C(14)−C(15)	169(2)	C(20)−C(19)−Pt(1)	171.2(12)
C(19)−C(20)−C(21)	169(2)		

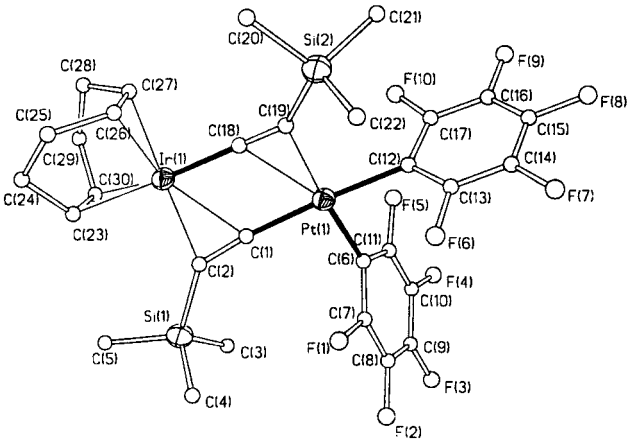

Figure 2. View of the molecular structure of the anion complex **3c**, showing the atom-numbering scheme.

(9) Å for Pt(1) and 2.308(8), 2.186(9) Å for Ir(1)] are comparable within experimental error. The η^2-metal acetylenic linkages are asymmetric, the M−C_β bonds ca. 0.1 Å (0.10 for Pt and 0.122 for Ir) being shorter than the corresponding M−C_α distances. This asymmetry has been previously found in related complexes,[6] and it would now seem to be characteristic of this particular

Chart 1

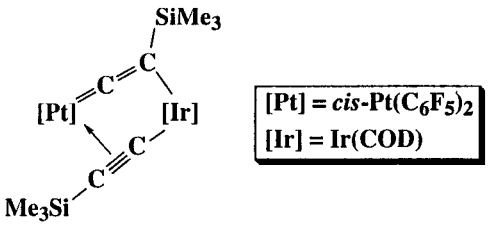

structural situation of the alkynyl ligands. In accordance with this structural fact, the M−C_α≡C_β fragments remain almost linear [174.6(7)°, 173.3(7)°] and the C_α≡C_β−Si units deviate significantly from linearity [136.9(7)°, 145.0(8)°], suggesting, as has been previously pointed out,[6d,g,h] a considerable vinylidene contribution to the bonding mode of the bridging alkynyl ligands (Chart 1). The opposite asymmetry (M−C_α < M−C_β) or more symmetrical η^2-metal acetylenic bonding interactions have usually been observed in complexes with chelating-type structural arrangements (M in-plane, tweezer-like and outside-plane, V-shaped),[2c,4,7] although we have also found some exceptions.[4,7d]

The Ir−(olefin) distances fall within the range of 2.117(9)−2.199(10) Å, with the two metal−carbon dis-

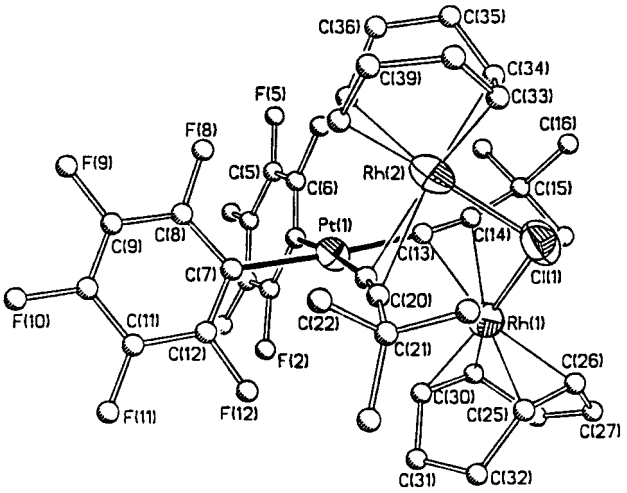

Figure 3. Molecular structure of the anion complex **4b**, showing the atom-numbering scheme.

tances trans to the C≡C triple bond shorter than those trans to the sp C_α carbon donor, thus revealing not only the asymmetric arrangement of the μ-C≡CSiMe$_3$ ligands but also the stronger trans influence of the σ-donor C_α carbon atom. Similar observations have previously been made on the basis of ^{195}Pt−^{31}P coupling constants.[6h]

For complex **4b** the unit cell contains 1.5 independent anions. The half anion sits on a crystallographic symmetry element. Both anions are essentially similar; therefore, the discussion will be limited to only one. The molecular structure of the trinuclear anion of **4b** is presented in Figure 3. This type of structure features a different behavior of the anionic substrates [*cis*-Pt(C$_6$F$_5$)$_2$(C≡CR)$_2$]$^{2-}$. In this case, the bis(alkynyl) fragment acts as a bridging diyne ligand (η^2:η^2) to two nearly identical "Rh(COD)" units. The structure is similar to the pentanuclear species **[PtRh$_4$X$_2$]**,[21] in which the tetraalkynylplatinate(II) anion acts as a tetradentate bridging ligand between two related cationic dirhodium "Rh$_2$(μ-X)(COD)$_2$" units. The anion contains two pseudo-square-planar Rh(I) units sharing a common bridged chlorine atom [Rh(1,2)−Cl(1) 2.421(4), 2.420(4) Å; Rh(1)−Cl−Rh(2) 98.60(14)°]. The two chelating diolefin ligands (COD) are not identical, but all the rhodium−carbon separations are very similar [2.11(2)−2.16(2) Å], in agreement with the values indicated in the literature.[21,24,25] Both rhodium centers complete their coordination, being η^2-bonded to a 3-platinadiyne bridging building block "*cis*-(C$_6$F$_5$)$_2$Pt(C≡C^{t}Bu)$_2$". In this fragment the coordination around Pt(1), including bond lengths and angles, is similar to those found in other heteropolynuclear bis(alkynyl)platinum compounds.[4,7d,17,21] As for **2a**, the most remarkable feature is that the η^2-interactions to the Rh atom show asymmetry opposite that found in **3c**: the Rh−C_α distances [2.238(13), 2.266(12) Å] are considerably shorter than the corresponding Rh−C_β [2.500(14), 2.547(14) Å]. The parameters of the acetylenic fragments [C≡C 1.21(2) Å; Pt−C_α≡C_β 172.2(12)°, 171.2(12)°; C_α≡C_β−C(^{t}Bu) 169-(2)°] are similar to those found in **[PtRh$_4$X$_2$]**[21] and in **2a**. The π-complexed Rh atoms are located in a pseudo-trans arrangement with respect to the platinum coordination plane, resulting in rather long Pt−Rh(1,2) [3.238(1) and 3.206(1) Å] and Rh(1)−Rh(2) [3.670(1) Å] separations, which exclude any significant metal−metal bonding interaction.

Spectroscopic Studies (IR, NMR). In accordance with previous observations,[11] the ν(C≡C) for the binuclear platinum rhodium compounds **2** (1940−2044 cm^{-1}) and, particularly, the $\Delta\nu$(C≡C) shift in relation to the precursors **1** (∼60 cm^{-1}) are in keeping with a chelating-type arrangement. In contrast, the formation of complex **3c** is accompanied by a considerably larger shift of the ν(C≡C) to lower frequencies (1868, 1823 cm^{-1}, $\Delta\nu$(C≡C)$_{average}$ 173 cm^{-1}), clearly reflecting stronger η^2-M−alkyne interactions with this type of arrangement of both alkynyl ligands.

Complex **3c**, like many other examples that have this σ/π structural formulation,[6a−i,q,11,12,16a] is dynamic and undergoes an intramolecular exchange of both alkynyl groups within the dimetallic framework that is rapid on the NMR time scale at room temperature. Thus, at 16 °C it shows only one proton and carbon olefinic resonances due to the COD ligands, only one type of C$_6$F$_5$ ligand (AA′MXX′ system), and only one set of C≡CSiMe$_3$ signals (^{1}H, ^{13}C, and ^{19}F NMR), evidencing an apparent overall C_{2v} symmetry. Lowering the temperature produces a broadening of CH═ and SiMe$_3$ resonances in the proton spectra and of the *o*-F signals (broadening of *p*-F and *m*-F is also observed) in the ^{19}F NMR spectra, which eventually split in each case into two separate signals (1:1 ratio) at low temperature (−50 °C). Using the coalescence temperatures for the olefinic protons (253 K), SiMe$_3$ (230 K), and *o*-F (253 K), a similar Gibbs activation barrier[26] is obtained ($\Delta G^\#$ 10.84, 11.86, and 11.13 kcal·mol^{-1}, respectively), suggesting that all these signals are involved in the same dynamic process. However, the low-temperature NMR patterns indicate that only the intramolecular C≡CSiMe$_3$ migration between the metal centers is frozen at low temperature (−50 °C). For a rigid puckered dimer one should expect to observe four proton and carbon olefinic resonances for the chelating COD ligand and four different fluorine signals (endo and exo of each C$_6$F$_5$ group) in the *o*-F region. Therefore, the reduced number of observable HC═ (^{1}H δ 4.89, 3.55; ^{13}C δ 62.3, 58.1) and *o*-F signals (−114.21, $^3J_{Pt-o-F}$ = 373 Hz, 2 *o*-F trans to σ-C≡C; −116.26, $^3J_{Pt-o-F}$ = 520 Hz, 2 *o*-F trans to η^2-C≡C) clearly indicates that a very fast inversion of the central dimetallacycle is taking place, even at 223 K, to account for the apparent time-averaged plane of symmetry.

Fluxional behavior for binuclear chelating platinum rhodium compounds **2a**−**2c** is also evident. At ambient temperature their proton and fluorine NMR spectra correspond to species for which the central Pt(C≡C)$_2$Rh framework is, on the NMR time scale, an average plane (see Experimental Section for data). The observed apparent overall C_{2v} symmetry is consistently explained[6i,7d,11,17] by means of a fast exchange of the "Rh-

(24) (a) Ibers, J. A.; Snyder, R. G. *Acta Crystallogr.* **1962**, *15*, 923. (b) Ridder, D. J. A.; Imhoff, P. *Acta Cristallogr.* **1994**, *C50*, 1569.

(25) (a) Feiken, N.; Pregosin, P.; Trabesinger, G. *Organometallics* **1998**, *17*, 4510. (b) Polborn, K.; Severin, K. *Eur. J. Inorg. Chem.* **1998**, 1187.

(26) Günther, H. *NMR Spectroscopy*; Wiley: New York, 1980; p 241.

(COD)" unit below and above the 3-platina-1,4-diyne fragments "$(C_6F_5)_2Pt(C{\equiv}CR)_2$", as is shown in eq 2.

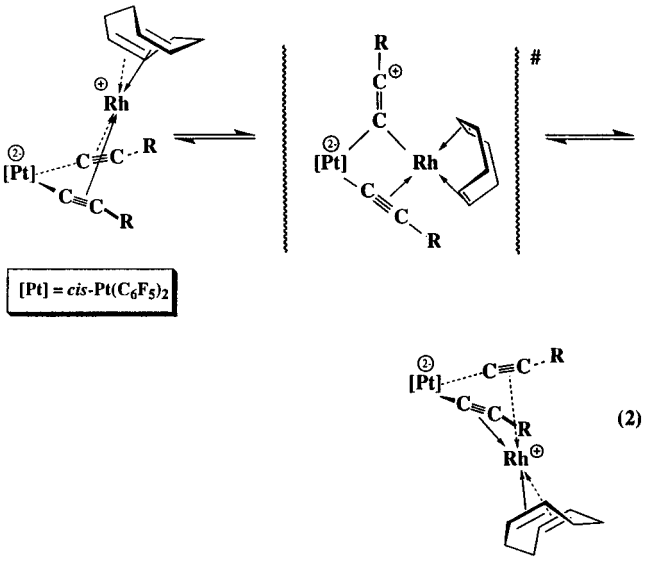

(2)

As has been previously suggested,[6i] the formal inversion of the central PtC_4Rh core could occur through intermediate species (or transition state) with one or both C≡CR symmetrically bridging the two metal centers. According to this proposal, the process should be more favorable for the phenylethynyl derivative **2a**, as the positive charge developed at the β-position should be stabilized by conjugation with the π-electron density of the phenyl group. This is further supported by the fact that for complex **2a** both the ^{19}F and proton NMR spectra did not change significantly over the observed temperature range (16 to −50 °C in $CDCl_3$ or 16 to −90 °C in acetone-d_6), indicating that the dynamic process has a very low energetic barrier. In contrast, for complexes **2b** and **2c** upon cooling at low temperature (below −50 °C in acetone-d_6) usual line broadening takes place and the signals due to olefinic protons for complex **2c** and to *o*-F for both complexes finally split into two different resonances at −80 °C (δ −114.11, −114.63 *o*-F; $\Delta G_{198}^{\#} \approx 9.15$ kcal·mol^{-1}; **2b**. δ 4.79, 4.60 olefinic protons; $\Delta G_{213}^{\#} \approx 10.27$ kcal·mol^{-1} and δ −114.21, −114.73 *o*-F; $\Delta G_{200}^{\#} = 9.25$ kcal·mol^{-1}; **2c**).

Interestingly, dissolution of crystals of the trinuclear complexes **4b** and **4c** occurs with partial dissociation according to eq 3, to yield an equilibrium mixture of compounds **4b**,**c** with the related **2b**,**c** and the corresponding rhodium dimer $[Rh(\mu\text{-Cl})(COD)]_2$, $[Rh_2]$. Similar final ratios **4**/**2**/$[Rh_2]$ are observed by monitoring equimolar mixtures of **1b**,**c** and the rhodium chloride dimer $[Rh_2]$, suggesting that **4b** and **4c** formed in situ rapidly equilibrate with the thermodynamically more stable dimers **2b** and **2c**, respectively. In each case, the final ratio of the three complexes **4**/**2**/$[Rh_2]$, which is obtained by the integration of the olefinic signals of 1,5-COD in the three species, strongly depends on the solvent (see Experimental Section). However, in the range observed (−80 to 50 °C), the temperature has very little influence on the extent of the dissociation in both species. We note that this equilibration process requires only small changes in the central bridging framework.

$$[\{cis\text{-}Pt(C_6F_5)_2(\mu\text{-}C{\equiv}CR)_2\}\{Rh_2(\mu\text{-}Cl)(COD)_2\}]^- \rightarrow \underset{\textbf{4b,c}}{} [cis\text{-}Pt(C_6F_5)_2(\mu\text{-}C{\equiv}CR)_2Rh(COD)\}]^- + \underset{\textbf{2b,c}}{} 1/2[Rh(\mu\text{-}Cl)(COD)]_2 \quad (3)$$

Spectroscopic data for **4b** and **4c** are easily extracted from these mixtures. Only a single olefinic resonance was seen at 16 °C for both complexes in the ^1H NMR spectra, and the ^{19}F NMR spectra at the same temperature exhibit a typical AA′MXX′ system, consistent with the existence of mirror planes on the three metal centers and, in the case of the rhodium atoms, with an additional time-averaged plane which equilibrates both halves (trans to Cl and trans to acetylenic unit) of the COD ligands. This latter equilibration could be related to the equilibrium shown in eq 3, which presumably requires the involvement of three-coordinated rhodium species resulting from cleavage of either rhodium−chloride and/or rhodium−η^2-alkyne linkages. However, the ^1H phase-sensitive NOESY spectra at room temperature of **4b** in $CDCl_3$ and **4c** in acetone-d_6 do not show cross negative peaks correlating the olefinic signals of **4** with those in **2** and $[Rh_2]$, thus suggesting that the intermolecular exchange between these species is very slow on the NMR time scale. In fact, coalescence of the three olefinic signals is not reached up to the maximum temperature registered (∼50 °C). For **4c**, the *ortho*-fluorine signal (δ −114.69, acetone-d_6) broadens as the temperature is lowered, coalesces at ca. −73 °C, and finally splits into two very broad humps at −80 °C (δ −112.7, −117.0). However, in the ^1H NMR spectrum the broad singlet olefinic signal at δ 4.55 attributed to **4c** does not change within the observed range (−80 to 50 °C), indicating that it is still dynamic on the NMR time scale. For **4b** the *o*-F resonance broadens by lowering the temperature, but does not split. The coalescence was very near to the lower accessible temperature limit (ca. −80 °C). In contrast, its proton spectrum displays a marked dependence on the temperature. Thus, the broad olefinic signal of **4b** (δ 4.62) coalesces at ca. −30 °C ($\Delta G_{243}^{\#} = 11.1$ kcal·mol^{-1}) and splits at −50 °C into two broad proton resonances (δ 4.91 and 4.20). These signals belong to protons of different C=C bonds (trans to Cl δ 4.20 and trans to acetylenic δ 4.91) since a correlation ^1H-COSY spectrum at −50 °C confirms that they are not coupled. At the same temperature, its ^{13}C NMR also displays, in addition to alkynyl carbon signals (C_α/C_β 81.1/105.2), only two olefinic (δ 75.9, 74.9) and two aliphatic carbon resonances (δ 30.0, 29.9). This suggests the existence of a fast intramolecular process, presumably a rapid ring inversion of the central six-membered Pt(acetylenic)-Rh_2Cl, which equilibrates the endo and exo CH= units in the diolefin. This process cannot be frozen even at −80 °C. Below −50 °C, the olefinic proton signals broaden again, but only the high-frequency signal (trans to acetylenic fragment) disappears into the baseline at −80 °C.

Experimental Section

General methods and instrumentation have been described previously.[21] All coupling constants are given in hertz. ^1H-

COSY and ^{1}H phase-sensitive NOESY spectra were recorded following literature methods.[27] $Q_2[cis\text{-}Pt(C_6F_5)_2(C{\equiv}CR)_2]$ (Q = PPh_3Me, R = Ph;[28] Q = NBu_4, R = ^{t}Bu,[28] $SiMe_3$[17a]), $[Rh(\mu\text{-}Cl)(COD)]_2$,[29] $[Ir(\mu\text{-}Cl)(COD)]_2$.[30] and $AgClO_4$[31] were prepared by published methods.

Preparation of Q[{*cis*-Pt(C$_6$F$_5$)$_2$(μ-1κC^{α}:η^2-C≡CR)$_2$}Rh(COD)] (Q = PPh$_3$Me, R = Ph 2a; Q = NBu$_4$, R = ^{t}Bu 2b, SiMe$_3$ 2c). A yellow solution of $[Rh(\mu\text{-}Cl)(COD)]_2$ (0.0476 g, 0.096 mmol) in Et_2O (40 mL) was treated with $AgClO_4$ (0.040 g, 0.190 mmol), and the mixture was stirred for 1 h at room temperature and then filtered through Kieselgurh. To the resulting yellow solution, which probably contains $[Rh(COD)(Et_2O)_2](ClO_4)$, was added $(PPh_3Me)_2[cis\text{-}Pt(C_6F_5)_2(C{\equiv}CPh)_2]$ (0.240 g, 0.190 mmol), and a white suspension (PPh_3MeClO_4) in a deep orange solution immediately formed. After stirring for 30 min, the suspension was filtered through Kieselgurh and the filtrate evaporated to dryness. Treatment of the resulting oily residue with 5 mL of cold hexane afforded **2a** (orange, 70% yield).

Complexes **2b** and **2c** (orange solids) were obtained similarly starting from $(NBu_4)_2[cis\text{-}Pt(C_6F_5)_2(C{\equiv}CR)_2]$ (R = ^{t}Bu, 0.250 g, 0.21 mmol **2b**; R = $SiMe_3$, 0.300 g, 0.25 mmol **2c**) and $[Rh(COD)(Et_2O)_2](ClO_4)$ (**2b** 0.23 mmol, 64% yield; **2c** 0.27 mmol, 88% yield).

Data for 2a. Anal. Calcd for $C_{55}F_{10}H_{40}PPtRh$: C, 54.15; H, 3.30. Found: C, 53.96; H, 3.17. Λ_M: 84.5 $\Omega^{-1}\cdot cm^2\cdot mol^{-1}$. MS FAB(−): *m*/*z* = 942 [M] 100; 835 [M − COD + 1] 15; 774 [M − C_6F_5 − 1] 9; 733 $[Pt(C_6F_5)_2(C_2Ph)_2 + 2]$ 15; 630 $[Pt(C_6F_5)_2(C_2Ph)]$ 27; 529 $[Pt(C_6F_5)_2]$ 32; 510 $[Pt(C_6F_5)(C_6F_4)]$ 57; 362 $[Pt(C_6F_5)]$ 43. IR (cm^{-1}): ν(C≡C) 2024(m br); $\nu(C_6F_5)_{x-sensitive}$ 798 (s), 790 (s). ^{1}H NMR (acetone-d_6, δ): at 16 °C, 7.84, 7.54, 7.29 (m, Ph, PPh_3Me, C_2Ph, 25H); 4.43 (s, CH═, COD, 4H); 3.22 (d, $^2J_{P-H}$ = 14.0, $PPh_3(CH_3)$); 2.47 (s br, $CH_2<$, COD, 4H); 1.84 (d, J_{H-H} = 7.3, $CH_2<$, COD, 4H). A similar but slightly broader pattern was observed at −75 °C: 7.97, 7.85, 7.57, 7.34 (m, Ph, PPh_3Me, C_2Ph, 25 H); 4.34 (v br, CH═, COD, 4H); 3.32 (d, $^2J_{P-H}$ = 14.4, $PPh_3(CH_3)$); 2.43 (v br, $CH_2<$, COD, 4H); 1.82 (d, J_{H-H} = 7.7, $CH_2<$, COD, 4H). ^{19}F NMR (acetone-d_6, δ): at 16 °C, −114.76 (d, $^3J_{Pt-o-F}$ = 395.1, 4 *o*-F); −167.31 (m, 4 *m*-F, 2 *p*-F). A similar pattern was observed at −75 °C: −114.65 (s, $^3J_{Pt-o-F}$ = 402.9, 4 *o*-F); −165.87 (m, 4 *m*-F, 2 *p*-F). ^{13}C NMR ($CDCl_3$, δ): at −50 °C, 147.3 (dd, $^1J_{C-F}$ = 227, $^2J_{C-F}$ = 25), 135.7 (dm) (C_6F_5); 134.8 (s, *p*-C, PPh_3Me); 132.4 (d, $^3J_{P-C}$ = 10.7, *m*-C, PPh_3Me); 132.1 (s, Ph,C_2Ph); 129.9 (d, $^2J_{P-C}$ = 12.9, *o*-C, PPh_3Me); 127.8, 127.0, 126.4 (s, Ph, C_2Ph); 118.0 (d, $^1J_{P-C}$ = 89, *i*-C, PPh_3Me); 109.6 (s br, $^1J_{Pt-C}$ = 856 Hz, C_α, $C_\alpha{\equiv}C_\beta$-Ph); 99.4 (s, $^2J_{Pt-C}$ = 254 Hz, C_β, $C_\alpha{\equiv}C_\beta$Ph); 81.0 (s br, CH═, COD); 30.8 (s br, $CH_2<$, COD); 9.4 (d, $^1J_{P-C}$ = 57, $PPh_3(CH_3)$).

Data for 2b. Anal. Calcd for $C_{48}F_{10}H_{66}NPtRh$: C, 50.35; H, 5.81; N, 1.22. Found: C, 50.19; H, 6.40; N, 1.39. Λ_M: 76.6 $\Omega^{-1}\cdot cm^2\cdot mol^{-1}$. MS FAB(−): *m*/*z* = 902 [M] 100; 794 [M − COD] 13; 692 $[Pt(C_6F_5)_2(C_2{}^tBu)_2 + 1]$ 22; 611 $[Pt(C_6F_5)_2(C_2{}^tBu) + 1]$ 20; 530 $[Pt(C_6F_5)_2 + 1]$ 20; 511 $[Pt(C_6F_5)(C_6F_4) + 1]$ 47; 362 $[Pt(C_6F_5)]$ 35%. IR (cm^{-1}): ν(C≡C) 2044 (m), 2017 (m); $\nu(C_6F_5)_{x-sensitive}$ 783 (vs), 776 (vs). ^{1}H NMR (acetone-d_6, δ): at 16 °C, 4.76 (s br, CH═, COD, 4H); 3.46 (m, N−CH_2−, NBu_4, 8H); 2.52 (br, $CH_2<$, COD, 4H); 1.84 (m, $CH_2<$ (COD) and −CH_2− (NBu_4), 12H); 1.43 (m, −CH_2−, NBu_4, 8H); 1.24 (s, $C(CH_3)_3$, 18H); 0.98 (t, −CH_3, NBu_4, 12H). At −80 °C a similar pattern is observed with the exception of the signal due to the olefinic protons of the COD, which practically coalesces: 4.66 (v br, CH═, COD, 4H); 3.41 (s br, N−CH_2−, NBu_4, 8H); 2.46 (m br, $CH_2<$, COD, 4H); 1.74 (m, $CH_2<$ (COD) and −CH_2− (NBu_4), 12H); 1.32 (m, −CH_2−, NBu_4, 8H); 1.18 (s, $C(CH_3)_3$, 18H); 0.89 (s br, −CH_3, NBu_4, 12H). ^{19}F NMR (acetone-d_6, δ): at 16 °C, −114.44 (dm, $^3J_{Pt-o-F}$ = 400.9, 4 *o*-F); −167.82 (m, 4 *m*-F); −168.40 (t, 2 *p*-F). The signal due to the *o*-F of the C_6F_5 groups coalesces at ca. −75 °C ($\Delta G_{198}^{\#} \approx 9.15$ kcal·mol^{-1}), splitting into two broad signals at −80 °C: −114.11 (2 *o*-F), −114.63 (2 *o*-F) (v br, platinum satellites are observed but are not well resolved); −166.29 (m, 4 *m*-F, 2 *p*-F). ^{13}C NMR ($CDCl_3$, δ): at −50 °C, 147.5 (dd, $^1J_{C-F}$ = 220, $^2J_{C-F}$ = 24), 135.7 (dm, $^1J_{C-F} \approx 250$), 134.8 (dm, $^1J_{C-F} \approx 244$) (C_6F_5); 109.1 (s, $^2J_{Pt-C} \approx 240$, C_β, $C_\alpha{\equiv}C_\beta{}^tBu$); 95.0 (s br, $^1J_{Pt-C} \approx 825$ Hz, C_α, $C_\alpha{\equiv}C_\beta{}^tBu$); 75.7, 73.8 (br, CH═, COD); 58.1 (s, N−CH_2−$(CH_2)_2$−CH_3); 32.5 (s, $C(CH_3)_3$); 31.0 (br, $CH_2<$, COD); 30.5 (s, CMe_3); 23.2, 19.3 (s, N−CH_2−$(CH_2)_2$−CH_3); 13.5 (s, N−$(CH_2)_3$−CH_3).

Data for 2c. Anal. Calcd for $C_{46}F_{10}H_{66}NPtRhSi_2$: C, 46.93; H, 5.65; N, 1.19. Found: C, 46.72; H, 6.01; N, 1.43. Λ_M: 115.2 $\Omega^{-1}\cdot cm^2\cdot mol^{-1}$. MS FAB(−): *m*/*z* = 934 [M] 100; 836 [M − C_2SiMe_3 − 1] 4; 626 $[Pt(C_6F_5)_2(C_2SiMe_3)]$ 16; 362 $[Pt(C_6F_5)]$ 12. IR (cm^{-1}): ν(C≡C) 1965 (vs), 1940 (vs); $\nu(C_6F_5)_{x-sensitive}$ 786 (vs), 777 (vs). ^{1}H NMR (acetone-d_6, δ): at 16 °C, 4.78 (s br, CH═, COD, 4H); 3.46 (m, N−CH_2−, NBu_4, 8H); 2.56 (br, $CH_2<$, COD, 4H); 1.85 (m, $CH_2<$ (COD) and −CH_2− (NBu_4), 12H); 1.44 (m, −CH_2−, NBu_4, 8H); 0.98 (t, −CH_3, NBu_4, 12H); 0.18 (s, $SiMe_3$, 18H). The signal due to the olefinic protons of the COD coalesces at ca. −60 °C ($\Delta G_{213}^{\#} \approx 10.27$ kcal·mol^{-1}), splitting into two broad singlets at lower temperature [e.g., at −80 °C, 4.79 (2H), 4.60 (2H) (s br, CH═, COD); 3.41 (m br, N−CH_2−, NBu_4, 8H); 2.50 (4H), 1.96 (4H) (m br, $CH_2<$, COD); 1.74 (8H), 1.31 (8H) (m br, −CH_2−, NBu_4); 0.89 (m, −CH_3, NBu_4, 12H); 0.13 (s, $SiMe_3$, 18H)]. ^{19}F NMR (acetone-d_6, δ): at 16 °C, −114.51 (dm, $^3J_{Pt-o-F}$ = 386, 4 *o*-F); −167.42 (m, 4 *m*-F, 2 *p*-F)]. The signal due to the *o*-F of the C_6F_5 groups coalesces at ca. −73 °C ($\Delta G_{200}^{\#} \approx 9.25$ kcal·mol^{-1}) and, finally, splits in two broad singlets at −80 °C: −114.21 (s br, $^3J_{Pt-o-F}$ = ≈ 340, 2 *o*-F), −114.73 (s br, $^3J_{Pt-o-F}$ = 380.6, 2 *o*-F); −165.55 (t, 2 *p*-F), −165.90 (m, 4 *m*-F). ^{13}C NMR ($CDCl_3$, δ): at 16 °C, 148.0 (dd, $^1J_{C-F}$ = 224, $^2J_{C-F}$ = 25), 135.8 (dm) (C_6F_5); a badly resolved signal at 134.4, which overlaps with one of the multiplets due to the carbon of C_6F_5 groups, is probably due to C_α: 101.7 (d, $^1J_{Rh-C}$ = 5.4, $^2J_{Pt-C} \approx 240$, C_β, $C_\alpha{\equiv}C_\beta SiMe_3$); 79.0 (d, $^1J_{Rh-C}$ = 12.6, CH═, COD); 58.8 (s, N−CH_2−$(CH_2)_2$−CH_3); 31.2 (s, $CH_2<$, COD); 23.8, 19.3 (s, N−CH_2−$(CH_2)_2$−CH_3); 13.5 (s, N−$(CH_2)_3$−CH_3); 1.9 (s, $^1J_{C-Si}$ = 55.5, $SiMe_3$). At −50 °C, 147.4 (dm, $^1J_{C-F}$ = 226), 135.4 (dm) (C_6F_5); 101.3 (s br, $^2J_{Pt-C} \approx 235$, C_β, $C_\alpha{\equiv}C_\beta SiMe_3$); 78.0 (v br, CH═, COD); 58.1 (s, N−CH_2−$(CH_2)_2$−CH_3); 31.0 (v br, $CH_2<$, COD); 23.3, 19.3 (s, N−CH_2−$(CH_2)_2$−CH_3); 13.5 (s, N−$(CH_2)_3$−CH_3); 1.6 (s, $^1J_{C-Si}$ = 55.3, $SiMe_3$).

Reactions of Q$_2$[*cis*-Pt(C$_6$F$_5$)$_2$(C≡CR)$_2$] (Q = PPh$_3$Me, R = Ph; Q = NBu$_4$, R = ^{t}Bu, SiMe$_3$) with [M(μ-Cl)(COD)]$_2$ (M = Rh, Ir). All the reactions were carried out treating suspensions of $[M(\mu\text{-}Cl)(COD)]_2$ (M = Rh, Ir) in 20 mL of acetone at −20 °C with $Q_2[cis\text{-}Pt(C_6F_5)_2(C{\equiv}CR)_2]$ (Q = PPh_3Me, R = Ph; Q = NBu_4, R = ^{t}Bu, $SiMe_3$), varying only the reaction time. The resulting solutions were evaporated to dryness, and the residues thus obtained were treated with ca. 5 mL of cold EtOH.

Reactions of (PPh$_3$Me)$_2$[*cis*-Pt(C$_6$F$_5$)$_2$(C≡CPh)$_2$] with [Rh(μ-Cl)(COD)]$_2$. Starting from 0.0766 g (0.155 mmol) of $[Rh(\mu\text{-}Cl)(COD)]_2$ and 0.200 g (0.155 mmol) of $(PPh_3Me)_2[cis\text{-}Pt(C_6F_5)_2(C{\equiv}CPh)_2]$ (molar ratio Rh/Pt 2:1), and after 15 min of stirring, an orange solid identified (^{1}H NMR) as a mixture of **2a** and $[Rh(\mu\text{-}Cl)(COD)]_2$ (molar ratio 2.5:1) was obtained. Monitoring of the reaction by ^{1}H and ^{19}F NMR spectroscopies reveals that no other product is formed.

An orange solid identified as **2a** was also obtained when the reaction was performed with 0.0287 g (0.058 mmol) of $[Rh(\mu\text{-}Cl)(COD)]_2$ and 0.150 g (0.117 mmol) of $(PPh_3Me)_2[cis\text{-}Pt(C_6F_5)_2(C{\equiv}CPh)_2]$ (molar ratio Rh/Pt 1:1, 15 min, 81% yield).

(27) Braun, S.; Kalinonowski, H.-O.; Berger, S. *100 and More Basic NMR Experiments*; VCH: Weinheim, Germany, 1996.

(28) Espinet, P.; Forniés, J.; Martínez, F.; Sotés, M.; Lalinde, F.; Moreno, M. T.; Ruiz, A.; Welch, A. J. *J. Organomet. Chem.* **1991**, *403*, 253.

(29) (a) Chatt, J.; Venanzi, L. M. *J. Chem. Soc.* **1957**, 4735. (b) Giordano, G.; Crabtree, R. H. *Inorg. Synth.* **1990**, *28*, 88.

(30) Herde, J. L.; Lambert, J. C.; Senoff, C. V. *Inorg. Synth.* **1974**, *15*, 18.

(31) Smith, G. F.; Ring, J. *J. Am. Chem. Soc.* **1937**, *59*, 1889.

Reactions of $(NBu_4)_2[cis\text{-}Pt(C_6F_5)_2(C{\equiv}C^tBu)_2]$ with $[Rh(\mu\text{-}Cl)(COD)]_2$. Starting from 0.063 g (0.128 mmol) of $[Rh(\mu\text{-}Cl)(COD)]_2$ and 0.151 g (0.128 mmol) of $(NBu_4)_2[cis\text{-}Pt(C_6F_5)_2(C{\equiv}C^tBu)_2]$ (molar ratio Rh/Pt 2:1), and after 40 min of stirring, an orange solid identified as $(NBu_4)[\{cis\text{-}Pt(C_6F_5)_2(\mu\text{-}1\kappa C^\alpha{:}\eta^2\text{-}C{\equiv}C^tBu)_2\}\{Rh_2(\mu\text{-}Cl)(COD)_2\}]$, **4b**, was obtained. Yield: 67%.

Complex **4b** was also obtained using the same reaction time and an equimolar Rh/Pt ratio: 0.063 mg (0.128 mmol) of $[Rh(\mu\text{-}Cl)(COD)]_2$ and 0.300 mg (0.256 mmol) of $(NBu_4)_2[cis\text{-}Pt(C_6F_5)_2(C{\equiv}C^tBu)_2]$. Yield: 56% (based on Rh).

Data for 4b. Anal. Calcd for $C_{56}ClF_{10}H_{78}NPtRh_2$: C, 48.34; H, 5.64; N, 1.01. Found: C, 48.16; H, 5.11; N, 1.02. Λ_M: 89.8 $\Omega^{-1}{\cdot}cm^2{\cdot}mol^{-1}$. MS FAB(−): m/z = 1148 [M − 1] 16; 902 [**2b**] 100; 794 [**2b** − COD] 15; 692 $[Pt(C_6F_5)_2(C_2{}^tBu)_2 + 1]$ 15; 611 $[Pt(C_6F_5)_2(C_2{}^tBu) + 1]$ 28; 565 $[Rh_2(COD)_3Cl]$ 31; 510 $[Pt(C_6F_5)(C_6F_4)]$ 90; 362 $[Pt(C_6F_5)]$ 41. IR (cm^{-1}): ν(C≡C) 2033 (s); $\nu(C_6F_5)_{x\text{-sensitive}}$ 788 (s), 780 (s). This complex dissociates in solution to give an equilibrium mixture of **2b**, **4b**, and $[RhCl(COD)]_2$. In $CDCl_3$, $K \approx 5.1 \times 10^{-2}$ $mol^{1/2}{\cdot}L^{-1/2}$ at 16 °C (e.g., for a $[\mathbf{4}]_{initial} = 1.47 \times 10^{-2}$ M, dissociation ca. 43%, molar ratio **4b**/**2b**/$[Rh(\mu\text{-}Cl)(COD)]$ 2.7:2:1). In acetone-d_6 complex **4b** dissociates to a lesser extent ($K \approx 9.2 \times 10^{-3}$ $mol^{1/2}{\cdot}L^{-1/2}$ at 16 °C, e.g., for a $[\mathbf{4b}]_{initial} = 1.35 \times 10^{-2}$ M, dissociation ca. 20%, molar ratio **4b**/**2b**/$[Rh(\mu\text{-}Cl)(COD)]$ 8:2:1). ^{1}H NMR (acetone-d_6, δ): at 16 °C, 4.62 (s br, CH═, COD); 3.46 (m, N−CH_2−, NBu_4); 2.48 (m br, CH_2<, COD); 1.84 (m, −CH_2−, NBu_4); 1.69 (d, J_{H-H} = 7.9, CH_2<, COD); 1.44 (m, −CH_2− (NBu_4) and s, $C(CH_3)_3$); 0.98 (t, −CH_3, NBu_4). A similar pattern was observed at 40 °C. By lowering the temperature, the olefinic signal broadens, coalesces at ca. −30 °C ($\Delta G_{243}^{\#}$ = 11.1 kcal·mol^{-1}), and splits at −50 °C: 4.91 (br, CH═, COD); 4.20 (br, CH═ protons of the COD ligand of **4b** overlapped with olefinic protons of $[RhCl(COD)]_2$ present due to the dissociation process); 3.42 (m, N−CH_2−, NBu_4); 2.42 (m br, CH_2<, COD); 1.77 (m, −CH_2−, NBu_4), 1.66 (m br, CH_2<, COD) (both of the signals are overlapped); 1.39 (m, −CH_2− (NBu_4) and s, $C(CH_3)_3$); 0.93 (t, −CH_3, NBu_4). At lower temperatures both olefinic signals (δ 4.91, 4.20) broaden again, and at ca. −80 °C the lower-field signal coalesces. ^{19}F NMR (acetone-d_6, δ): at 16 °C, −114.39 (dm, $^3J_{Pt-o-F}$ = 384, 4 *o*-F); −168.31 (m, 4 *m*-F); −168.98 (t, 2 *p*-F). At −80 °C, −114.30 (hump, 4 *o*-F); −167.05 (m, 4 *m*-F); −167.48 (t, 2 *p*-F). In all the spectra (^{1}H and ^{19}F NMR) signals due to **2b** and $[RhCl(COD)]_2$ are also observed. ^{13}C NMR (acetone-d_6, δ): at −50 °C, 147.0 (dm, $^1J_{C-F}$ = 226), 134.4 (dm, $^1J_{C-F} \approx 230$) (C_6F_5); 105.2 (s, $^2J_{Pt-C} \approx 270$, C_β, $C_\alpha{\equiv}C_\beta{}^tBu$); 81.1 (m, C_α, $C_\alpha{\equiv}C_\beta{}^tBu$); 75.9, 74.9 (m br, CH═, COD); 57.2 (s, N−CH_2−$(CH_2)_2$−CH_3); 31.5 (s, $C(CH_3)_3$); 31.0 (s, CMe_3); 30.3, 29.9 (br, CH_2<, COD); 22.6, 18.8 (s, N−CH_2−$(CH_2)_2$−CH_3); 12.6 (s, N−$(CH_2)_3$−CH_3). A small singlet at 31.7 [$C(CH_3)_3$, **2b**] is also observed.

Reactions of $(NBu_4)_2[cis\text{-}Pt(C_6F_5)_2(C{\equiv}CSiMe_3)_2]$ with $[Rh(\mu\text{-}Cl)(COD)]_2$. Starting from 0.075 g (0.152 mmol) of $[Rh(\mu\text{-}Cl)(COD)]_2$ and 0.183 g (0.152 mmol) of $(NBu_4)_2[cis\text{-}Pt(C_6F_5)_2(C{\equiv}CSiMe_3)_2]$ (molar ratio Rh/Pt 2:1), and after 10 min of stirring, an orange solid identified as $(NBu_4)[\{cis\text{-}Pt(C_6F_5)_2(\mu\text{-}1\kappa C^\alpha{:}\eta^2\text{-}C{\equiv}CSiMe_3)_2\}\{Rh_2(\mu\text{-}Cl)(COD)_2\}]$, **4c**, was obtained. Yield: 71%.

By using the same reaction time and a 1:1 Rh/Pt ratio (0.0225 g, 0.046 mmol, $[Rh(\mu\text{-}Cl)(COD)]_2$ and 0.110 g, 0.091 mmol, $(NBu_4)_2[cis\text{-}Pt(C_6F_5)_2(C{\equiv}CSiMe_3)_2]$) an orange solid which is identified as complex **2c** was obtained. Yield: 42%.

Data for 4c. Anal. Calcd for $C_{54}ClF_{10}H_{78}NPtRhSi_2$: C, 45.56; H, 5.52; N, 0.98. Found: C, 45.31; H, 5.28; N, 0.89. Λ_M: 78.1 $\Omega^{-1}{\cdot}cm^2{\cdot}mol^{-1}$. MS FAB(−): m/z = 1181 [M] 13; 934 [**2c**] 100; 724 $[Pt(C_6F_5)_2(C_2SiMe_3)_2 + 1]$ 12; 528 $[Pt(C_6F_5)_2 - 1]$ 24; 361 $[Pt(C_6F_5) - 1]$ 30. IR (cm^{-1}): ν(C≡C) 1966 (vs), 1952 (vs); $\nu(C_6F_5)_{x\text{-sensitive}}$ 789 (vs), 778 (vs). This complex dissociates in solution to give an equilibrium mixture of **2c**, **4c**, and $[RhCl(COD)]_2$. In $CDCl_3$, $K = 4.51 \times 10^{-1}$ $mol^{1/2}{\cdot}L^{-1/2}$ at 16 °C, e.g., for a $[\mathbf{4c}]_{initial} = 2.46 \times 10^{-2}$ M, dissociation ca. 82%, molar ratio **4c**/**2c**/$[Rh(\mu\text{-}Cl)(COD)]$ 1:4.5:2.25; in acetone-d_6, $K = 3.5 \times 10^{-2}$ $mol^{1/2}{\cdot}L^{-1/2}$ at 16 °C, e.g., for a $[\mathbf{4c}]_{initial} = 2.6 \times 10^{-2}$ M, dissociation ca. 38%, molar ratio **4c**/**2c**/$[Rh(\mu\text{-}Cl)(COD)]$ 3.3:2:1. ^{1}H NMR (acetone-d_6, δ): at 16 °C, 4.55 (s br, CH═, COD); 3.46 (m, N−CH_2−, NBu_4); 2.54 (m br, CH_2<, COD); 1.83 (m, −CH_2−, NBu_4); 1.74 (m, CH_2<, COD); 1.44 (m, −CH_2−, NBu_4); 0.98 (t, −CH_3, NBu_4), 0.25 (s, $SiMe_3$). At −80 °C the same pattern is observed: 4.45 (s br, CH═, COD); 3.42 (m, N−CH_2−, NBu_4); 2.46 (m br, CH_2<, COD); 1.75 (m br, −CH_2−, NBu_4); 1.32 (m br, CH_2< (COD) and −CH_2− (NBu_4)); 0.89 (t, −CH_3, NBu_4), 0.20 (s, $SiMe_3$). ^{19}F NMR (acetone-d_6, δ): at 16 °C, −114.69 (dm, $^3J_{Pt-o-F}$ = 384, 4 *o*-F); −168.04 (m, 4 *m*-F, 2 *p*-F). The signal due to the *o*-F coalesces at ca. −73 °C. At −80 °C, −112.7 (v br, 2 *o*-F), −117.0 (v br, 2 *o*-F); −166.54 (m, 4 *m*-F, 2 *p*-F). In all the spectra (^{1}H and ^{19}F NMR) signals due to **2c** and $[RhCl(COD)]_2$ are also observed. Due to the extent of the dissociation, the assignment of the ^{13}C NMR spectra in acetone-d_6 is rather uncertain: at 16 °C, 148.9 (dm, $^1J_{C-F} \approx 211$), 136.4 (dm) (C_6F_5); 128.1 (m), 97.8 (m) (C_α or C_β, $C_\alpha{\equiv}C_\beta$-$SiMe_3$, **2c** or **4c**); 79.5 (m), 78.7 (h) (CH═, COD, **2c** or **4c**); 59.3 (t, $^1J_{C-^{14}N}$ = 2.8, N−CH_2−$(CH_2)_2$−CH_3); 31.5 (s, CH_2<, COD); 24.3 (s, N−$(CH_2)_2$−CH_2−CH_3); 20.3 (t, $^2J_{C-^{14}N}$ = 1.3, N−CH_2−CH_2−CH_2−CH_3); 13.8 (s, N−$(CH_2)_3$−CH_3); 1.8 (s, $SiMe_3$). Two singlets at 31.9 (CH_2<, COD, **2c**) and 2.0 ($SiMe_3$, **2c**) are also observed.

Reactions of $(NBu_4)_2[cis\text{-}Pt(C_6F_5)_2(C{\equiv}CSiMe_3)_2]$ with $[Ir(\mu\text{-}Cl)(COD)]_2$. The reactions between $[Ir(\mu\text{-}Cl)(COD)]_2$ and $(NBu_4)_2[cis\text{-}Pt(C_6F_5)_2(C{\equiv}CSiMe_3)_2]$ in a 2:1 Ir/Pt ratio (0.100 g, 0.149 mmol, $[Ir(\mu\text{-}Cl)(COD)]_2$ and 0.180 g, 0.149 mmol, $(NBu_4)_2[cis\text{-}Pt(C_6F_5)_2(C{\equiv}CSiMe_3)_2]$; 10 min) or 1:1 Ir/Pt ratio (0.056 g, 0.084 mmol, $[Ir(\mu\text{-}Cl)(COD)]_2$ and 0.200 g, 0.164 mmol, $(NBu_4)_2[cis\text{-}Pt(C_6F_5)_2(C{\equiv}CSiMe_3)_2]$; 2 h) afforded a yellow solid, which was identified as $(NBu_4)[cis\text{-}Pt(C_6F_5)_2(\mu\text{-}1\kappa C^\alpha{:}\eta^2\text{-}C{\equiv}CSiMe_3)(\mu\text{-}2\kappa C^\alpha{:}\eta^2\text{-}C{\equiv}CSiMe_3)Ir(COD)]$, **3c**. Yields (based on Pt): 65 and 30.5%, respectively.

Complex **3c** can also be obtained in a very low yield (15%) by treatment of an equimolar amount of **1c** (0.170 g, 0.140 mmol) with a solution of $[Ir(COD)(acetone)](ClO_4)$, prepared from 0.0497 mg (0.074 mmol) of $[Ir(\mu\text{-}Cl)(COD)]_2$ and 0.0307 mg (0.148 mmol) of $AgClO_4$ and 1 h of stirring, in 20 mL of acetone. The resulting yellow solution, which was shown to contain **3c** by ^{19}F NMR, was evaporated to dryness and the residue treated with 20 mL of Et_2O to give a white suspension (NBu_4ClO_4) in a yellow solution. Filtration of the mixture, evaporation to dryness, and treatment of the resulting oily residue with cold hexane (∼10 mL) afforded 0.027 g of a yellow solid, which was identified as complex **3a**.

Data for 3c. Anal. Calcd for $C_{46}F_{10}H_{66}IrNPtSi_2$: C, 43.63; H, 5.25; N, 1.10. Found: C, 43.40; H, 4.87; N, 1.07. Λ_M: 71.1 $\Omega^{-1}{\cdot}cm^2{\cdot}mol^{-1}$. MS FAB(−): m/z = 1024 [M] 100; 926 [M − C_2SiMe_3] 35; 627 $[Pt(C_6F_5)_2(C_2SiMe_3) + 1]$ 78; 529 $[Pt(C_6F_5)_2]$ 48; 509 $[Pt(C_6F_5)(C_6F_4) - 1]$ 69; 362 $[Pt(C_6F_5)]$ 67. IR (cm^{-1}): ν(C≡C) 1868 (vs), 1823 (vs); $\nu(C_6F_5)_{x\text{-sensitive}}$ 796 (vs), 781 (s). ^{1}H NMR ($CDCl_3$, δ): at 16 °C, 4.27 (s br, CH═, COD, 4H); 3.15 (m br, N−CH_2−, NBu_4, 8H); 2.16 (m, CH_2<, COD, 4H); 1.89 (m, CH_2<, COD, 4H); 1.60 (8H), 1.40 (8H) (m, −CH_2−, NBu_4); 0.96 (t, −CH_3, NBu_4, 12H); −0.12 (s, $SiMe_3$, 18H). At −50 °C, 4.89 (2H), 3.55 (2H) (s br, CH═, COD); 3.15 (br, N−CH_2−, NBu_4, 8H); 2.14 (4H), 1.87 (4H) (s br, CH_2<, COD); 1.58 (8H), 1.33 (8H) (s br, −CH_2−, NBu_4); 0.91 (s br, −CH_3, NBu_4, 12H); −0.16 (9H), −0.20 (9H) (s, $SiMe_3$, the singlets overlapped partially). The signal due to the $SiMe_3$ protons coalesces between −40 and −50 °C ($\Delta G_{230}^{\#}$ = 11.86 kcal·mol^{-1}) and the signal due to the olefinic protons of the COD coalesces at −20 °C ($\Delta G_{253}^{\#}$ = 10.84 kcal·mol^{-1}). ^{19}F NMR ($CDCl_3$, δ): at 16 °C, −114.95 (d, $^3J_{Pt-o-F}$ = 444.5, 4 *o*-F); −166.29 (t, 2 *p*-F); −166.76 (m, 4 *m*-F). At −50 °C: −114.21 (d, $^3J_{Pt-o-F}$ = 373, 2 *o*-F trans to σ-C≡C); −116.26 (d, $^3J_{Pt-o-F}$ = 520, 2 *o*-F trans to η^2-C≡C); −165.23 (m br, 2 *p*-F); −166.30 (m, 4 *m*-F). The signal due to the *o*-F coalesces at ca. −20 °C and the corresponding one to the *p*-F at ca. −40 °C ($\Delta G_{253}^{\#}$ = 11.13

Table 2. Crystallographic Data and Structure Refinement Parameters for Complexes 2a, 3c, and 4b

	2a	3c	4b
empirical formula	$C_{55}H_{40}F_{10}PPtRh$	$C_{46}H_{66}NF_{10}Si_2PtIr$	$C_{87.5}H_{150.5}N_{1.5}Cl_3F_{15}Rh_3Pt_{1.5}$
fw	1219.84	1266.48	2216.31
a (Å)	21.921(4)	14.667(7)	36.629(7)
b (Å)	10.765(2)	18.946(6)	22.882(5)
c (Å)	19.765(4)	17.603(6)	28.661(6)
α (deg)	90	90	90
β (deg)	90	96.23(6)	127.21(3)
γ (deg)	90	90	90
volume (Å^3), *Z*	4664.14(2)	4862.79	19132(7)
wavelength (Å)	0.71073	0.71073	0.71073
temperature (K)	200	210	200
radiation	graphite monochomated Mo Kα	graphite monochromated Mo Kα	graphite monochromated Mo Kα
crystal system	orthorhombic	monoclinic	monoclinic
space group	$Pna2_1$	$P2_1/n$	$C2/c$
cryst dimens (mm)	0.3 × 0.2 × 0.3	0.4 × 0.3 × 0.2	0.70 × 0.45 × 0.36
abs coeff (mm^{-1})	3.462	5.73	2.848
transmission factors	0.975, 0.809	0.2927, 0.1418	1.000, 0.591
abs corr	Ψ scans	Ψ scans	Ψ scans
diffractometer	Siemens P4	Siemens Stoe AED2	Siemens P4
2*θ* range (deg)	4−50	4−47	4−48
no. of reflns collected	4827	7750	15430
no. of indep reflns	4495 (R_{int} = 0.074)	7163 (R_{int} = 0.028)	14788 (R_{int} = 0.021)
refinement method	full-matrix least-squares on F^2	full matrix leasts-squares on *F*	full-matrix least squares on F^2
goodness-of-fit on F^2 [a]	1.049	1.225	1.045
final *R* indices ($I > 2\sigma(I)$)[b]	R1 = 0.0681, wR2 = 0.1576	R1= 0.0383, wR = 0.0477	R1 = 0.0686, wR2 = 0.1832
R indices (all data)	R1 = 0.1050, wR2 = 0.1947	- -	R1 = 0.1208, wR2 = 0.2210

[a] Goodness-of-fit = $[\sum w(F_o^2 - F_c^2)^2/(n_{obs} - n_{param})]^{1/2}$. $w = [\sigma^2 (F_o) + (g_1P)^2 + g_2P]^{-1}$; $P = [\max(F_o^2; 0) + 2F_c^2]/3$. [b] R1 = $\sum(|F_o| - |F_c|)/\sum|F_o|$; wR2 = $[\sum w(F_o^2 - F_c^2)^2/\sum w(F_c^2)^2]^{1/2}$.

kcal·mol^{-1}). ^{13}C NMR ($CDCl_3$, *δ*): at 16 °C, 147.6 (dd, $^1J_{C-F}$ = 223, $^2J_{C-F}$ = 25), 135.9 (dm) (C_6F_5); 124.2, 112.85 (m, tentatively ascribed to C_α and C_β, $C_\alpha{\equiv}C_\beta SiMe_3$); 69.4 (v br, CH═, COD); 58.7 (s, N−*C*H$_2$−(CH$_2$)$_2$−CH$_3$); 31.9 (s, CH$_2$<, COD); 23.8, 19.6 (s, N−CH$_2$−(*C*H$_2$)$_2$−CH$_3$); 13.4 (s, N−(CH$_2$)$_3$−*C*H$_3$); 1.3 (s, SiMe$_3$, $^1J_{Si-C}$ = 54.6). At −50 °C, 147.1 (dm, $^1J_{C-F}$ = 226), 135.5 (dm, $^1J_{C-F}$ = 240) (C_6F_5); 122.9, 121.7, 117.5, 108.1 (m, tentatively ascribed to two C_α and two C_β, $C_\alpha{\equiv}C_\beta SiMe_3$); 62.3 (s br, CH═, COD); 58.1 (s br, CH═ (COD) and N−*C*H$_2$−(CH$_2$)$_2$−CH$_3$); 32.0, 31.5 (s br, CH$_2$<, COD, both of the signals are overlapped); 23.4, 19.4 (s, N−CH$_2$−(*C*H$_2$)$_2$−CH$_3$); 13.5 (s, N−(CH$_2$)$_3$−*C*H$_3$); 1.2, 1.0 (s br, SiMe$_3$).

X-ray Crystal Structure Determination of Complexes 2a, 3c, and 4b. Crystals of the three respective complexes were obtained at low temperature (−30 °C) by slow diffusion of hexane into chloroform solutions. Suitable crystals of **2a**, **3c**, or **4b** were selected and fixed with epoxy on top of glass fibers and transferred to the cold stream of the low-temperature device of automated four-circle difractometers Siemens P4 (**2a**, **4b**) or Siemens STOE AED2 (**3c**). For complex **2a**, the enantiomorph was chosen on the basis of the Flack parameter $x = -0.0163$ with esd 0.0183 (expected values are 0 for correct and +1 for inverted absolute structure). Crystallographic data and structure refinement parameters are shown in Table 2. Cell constants were calculated from 100 well-centered reflections with 2*θ* angles ranging from 16° to 30° (**2a**, **4b**) or 24 reflections with 2*θ* angles from 24° to 29° (**3c**). Data were collected at 200 K (**2a**, **4b**) or 210 K (**3c**) by the *ω*/2*θ* (**2a**), *ω*/*θ* (**3c**), or *ω* (**4b**) methods. Three check reflections measured at regular intervals showed no significant loss of intensity at the end of data collection in each case. An empirical absorption correction based on *ψ* scans was applied. The structures were solved by Patterson and Fourier methods. All non-hydrogen atoms were located in succeeding difference Fourier syntheses and refined with anisotropic thermal parameters except four C atoms in **2a**. No hydrogen atoms were added to the models. In complex **2a** the anisotropically refined C(1), C(6), C(13), and C(21) have large displacement parameters, and some disorder was observed. In complex **3c** the C(33) and C(34) atoms that belong to a NBu_4 group were refined as disordered over two positions. In the asymmetric unit of **4b** there are 1.5 molecules of the complex, the other half-molecule being generated by symmetry since the Pt atom and the bridging Cl are located in special positions. The half-molecule of NBu_4 is disordered over two positions, having two common carbon atoms, C(78) and C(79). N(2) and C(99), which belong to different NBu_4 units, occupy the same site at half-occupancy. Regions of electron density located at nonbonding distances were modeled as interstitial solvents: a molecule of $CHCl_3$, refined at half-occupancy with anisotropic thermal parameters, and three carbon atoms of a molecule of cyclohexane (the other carbon atoms being generated by a symmetry center) refined with isotropic thermal parameters at full occupancy. That makes one-third of each solvent molecule per formula unit. There are some peaks of electron density higher than 1 e/A^3 in the final map in all three structures (maximum 2.02 for **2a**, 1.16 for **3c**, and 1.69 for **4b**). In all cases, they are located very close to the heavy atoms or in the disordered solvent areas and have no chemical significance. All calculations were carried out using the programs SHELXTL-PLUS[32] and SHELXL-93.[33]

Acknowledgment. We wish to thank the Dirección General de Enseñanza Superior (Spain, Project PB 95-0003-CO2-01,02) and the Universidad de La Rioja (Project API-99/B17) for their financial support.

Supporting Information Available: Tables giving positional and thermal parameters and bond distances and bond angles for **2a**, **3c**, and **4b**. This material is available free of charge via the Internet at http://pubs.acs.org.

OM990314Z

(32) *SHELXTL-PLUS*, Software Package for the Determination of Crystal Structures, Release 4.0; Siemens Analytical X-ray Instruments Inc.: Madison, WI, 1990.

(33) Sheldrick, G. M. *SHELXL-93*, a Program for Crystal Structure Determination; University of Göttingen: Göttingen, Germany, 1993.